LA-UR- 96-3446 CONF-9608132--11

Title: **TWO-DIMENSIONAL MODELING OF MAGNETICALLY IMPLODED LINERS.**

RECEIVED
OCT 30 1996
OSTI

Author(s): W. L. Atchison, R. L. Bowers, J. H. Brownell, H. Lee, K. D. McLenithan, A. J. Scannapieco, W. R. Shanahan, M. G. Sheppard

Submitted to: Megagauss Conference
Sarov, Russia
5-9 August 1996

MASTER

Los Alamos
NATIONAL LABORATORY

Form No. 836 R5
ST 2629 10/91

DISTRIBUTION OF THIS DOCUMENT IS UNLIMITED HH

TWO-DIMENSIONAL MODELING OF MAGNETICALLY IMPLODED LINERS

W.L. Atchison, R.L. Bowers, J.H. Brownell, H. Lee, K.D. McLenithan, M. Rich, A.J. Scannapieco, W.R. Shanahan, and M.G. Sheppard
Los Alamos National Laboratory
Los Alamos, USA

Magnetically imploded massive cylindrical liner drivers have been studied in two-dimensions for low, intermediate and high energy pulsed power systems. The simulations have been carried out using a resistive Eulerian magnetohydrodynamics computational model which includes material strength, and models the interactions between the imploding liner and the electrode walls. The computations simulate the generation of perturbations and their subsequent growth during the implosion. At low energies a solid liner remains in the plastic regime, reaching an inner cylindrical target with velocities of a few mm per μs. At higher energies (where one-dimensional models predict implosion velocities of order 1 cm/μs or more) resistive heating of the liner results in melting, and the effects of magnetically driven instabilities become important. We discuss the two-dimensional issues which arise in these systems. These include: the onset of perturbations associated with the motion of the liner along the electrodes; the growth of instabilities in liquid layers; and the suppression of instability growth during the implosion by maintaining a solid inner layer. Studies have been made of liners designed for the Pegasus capacitor bank facility (currents in the 5 - 12 MA regime), and for the Procyon high explosive system (currents in the 20 MA regime). This work focus on the design and performance of the first Pegasus composite megabar liner experiment. LA-UR-96-1547.

Related Presentations

H. Lee, "Composite Liner Design to Maximize the Shock Pressure Beyond Megabars", Session #10, Magnetically Imploded Solid and Plasma Liners;

R.R. Bartsch, "Megabar Shock Generation with the Implosion of a Composite Liner", Session #9, Magnetically Imploded Liners;

W. Anderson, "Fabrication and Characterization of Aluminum Heavy Liners for the Pulsed Power Systems of the HEDP Program at Los Alamos", Session #9, Magnetically Imploded Liners.

M.G. Sheppard, "Multi Megagauss Field-Generation Using Capacitor Banks", Session #22, Non Destructive Production of High Magnetic Fields.

Composite megabar liner specifications assuming one-dimensional performance on Pegasus II (85 kV drive)

Composite liner design for 2-D pre-shot modeling:

$m_{liner} = 9$ g ; 8 g aluminum, $\Delta r = 0.06$ cm
1 g platinum, $\Delta r = 0.001$ cm
$r_0 = 4$ cm $\Delta z = 2$ cm
$v_{impact} \approx 1$ cm / µs $P_{shock} \approx 10$ Mb

Liner as fielded used a more conservative design to reduce Joule heating:

$r_0 = 3$ cm
$v_{impact} \approx 0.85$ cm / µs $P_{shock} \approx 8$ Mb

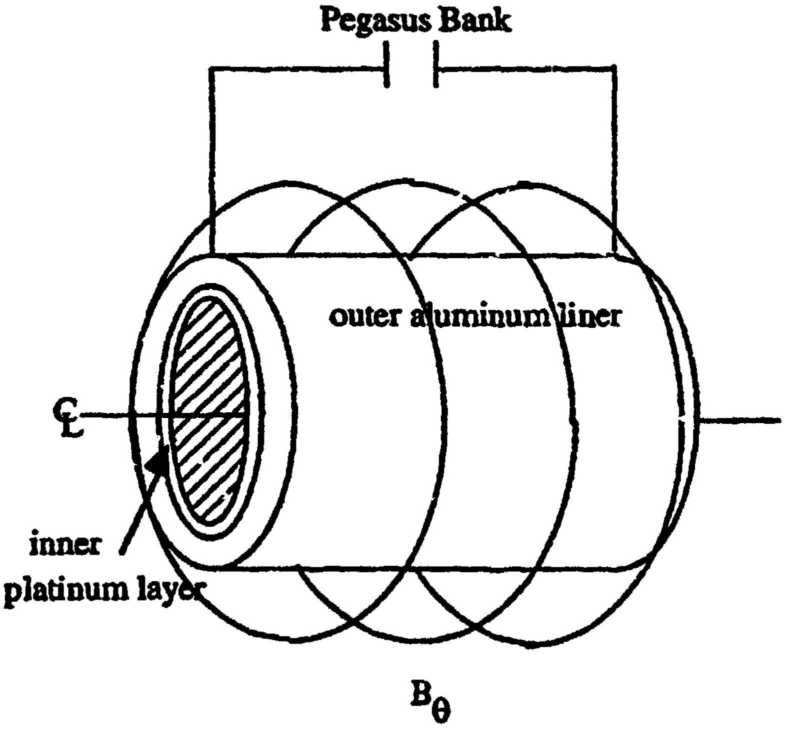

Current wave form for the 2-D models (upper), and for an upcoming experiment (lower). At right, liner radius versus time for the 4 cm model.

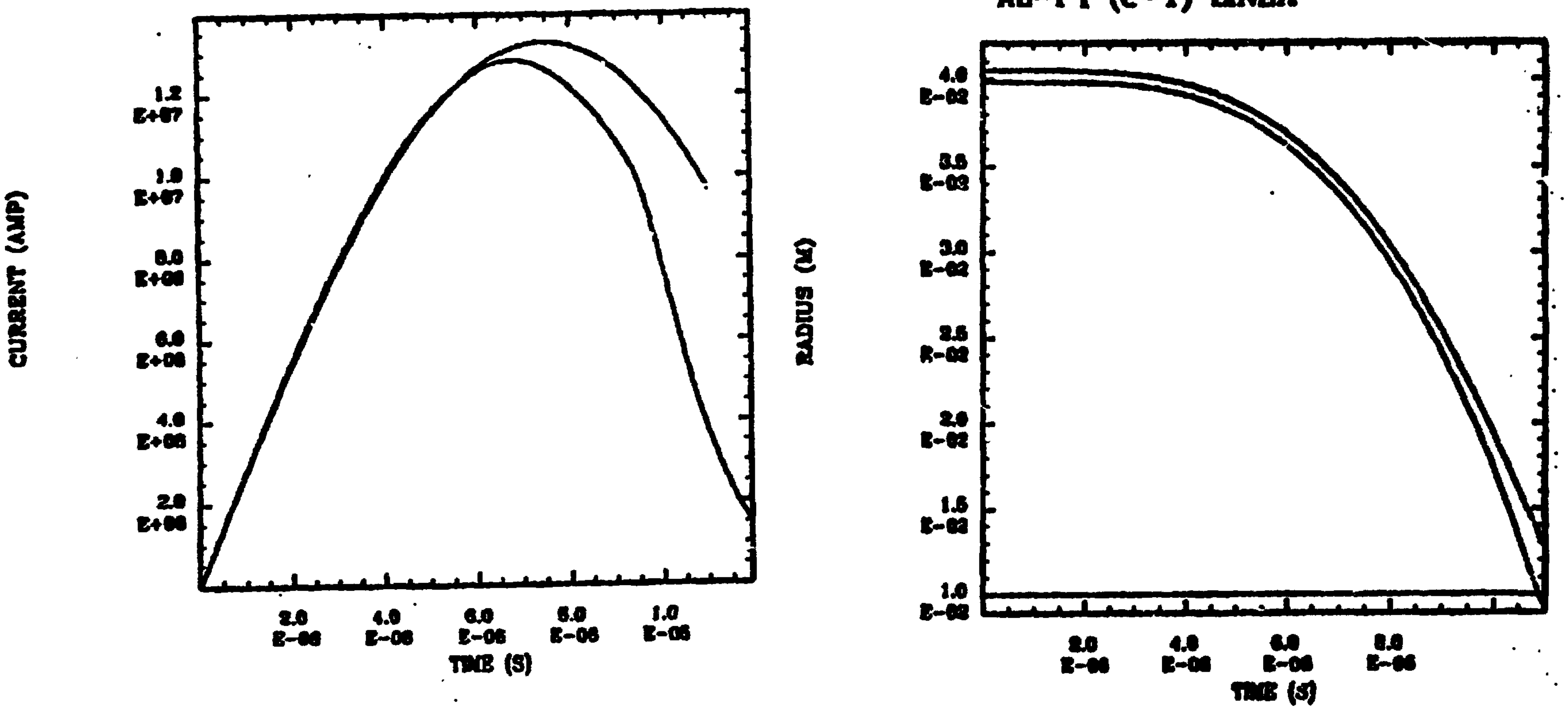

COMPARISON OF IMPLODING VELOCITIES

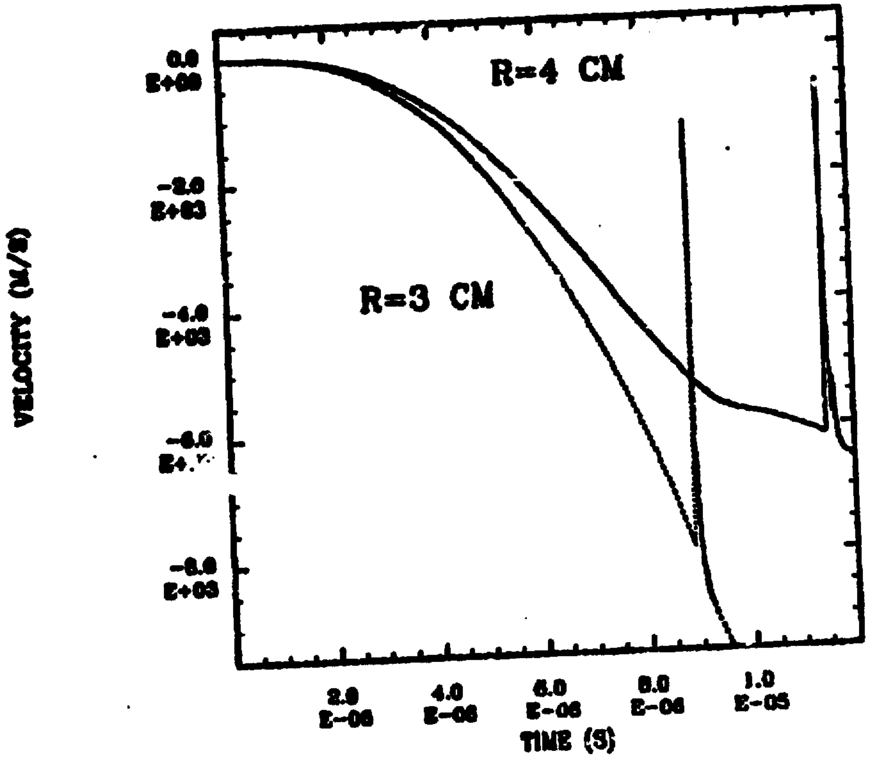

AL-PT (8-1) LINER

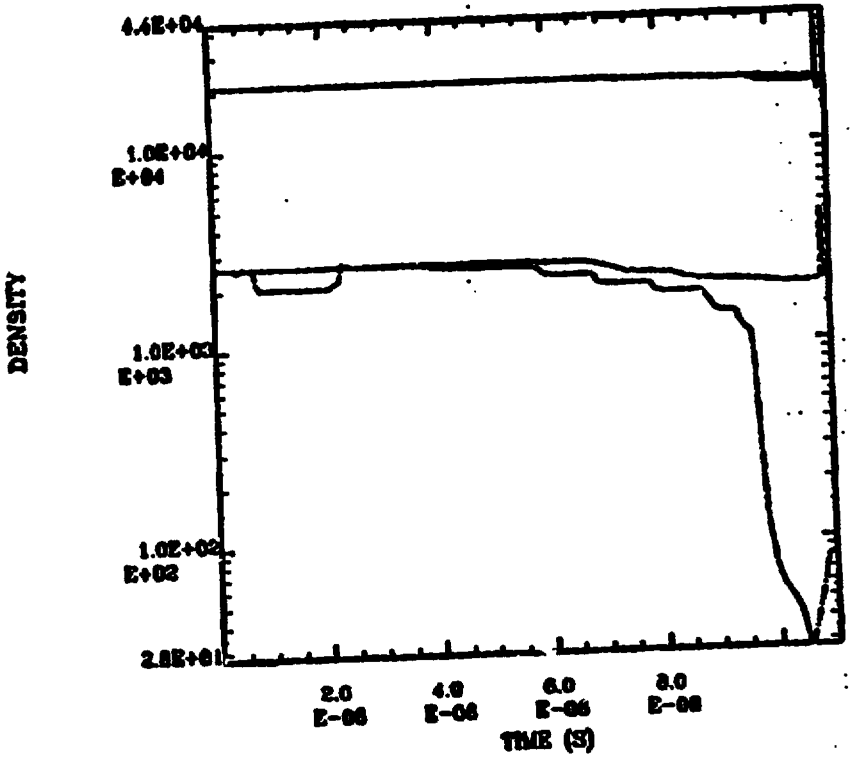

Approach used the capability which successfully produced the percision solid liner experiments

---

Computational algorithms included:

- hydrodynamics with internal contact discontinuities
- magnetic acceleration and resistive field diffusion
- 1-D current drive, including Pegasus bank damping resistor
- elastic-plastic strength model
- Steinberg-Guinan elastic-plastic strength parameters
- SESAME equations of state and electrical resistivites
- thermal conduction

Preliminary 2-D approach:

- current capabilities make it impractical to accurately model the thin platinum layer

$$\frac{\text{distance of radial travel}}{\text{platinum thickness}} = \frac{2.5\ cm}{.001\ cm} = 2500$$

- eliminate platinum layer; model 9 g pure aluminum liner

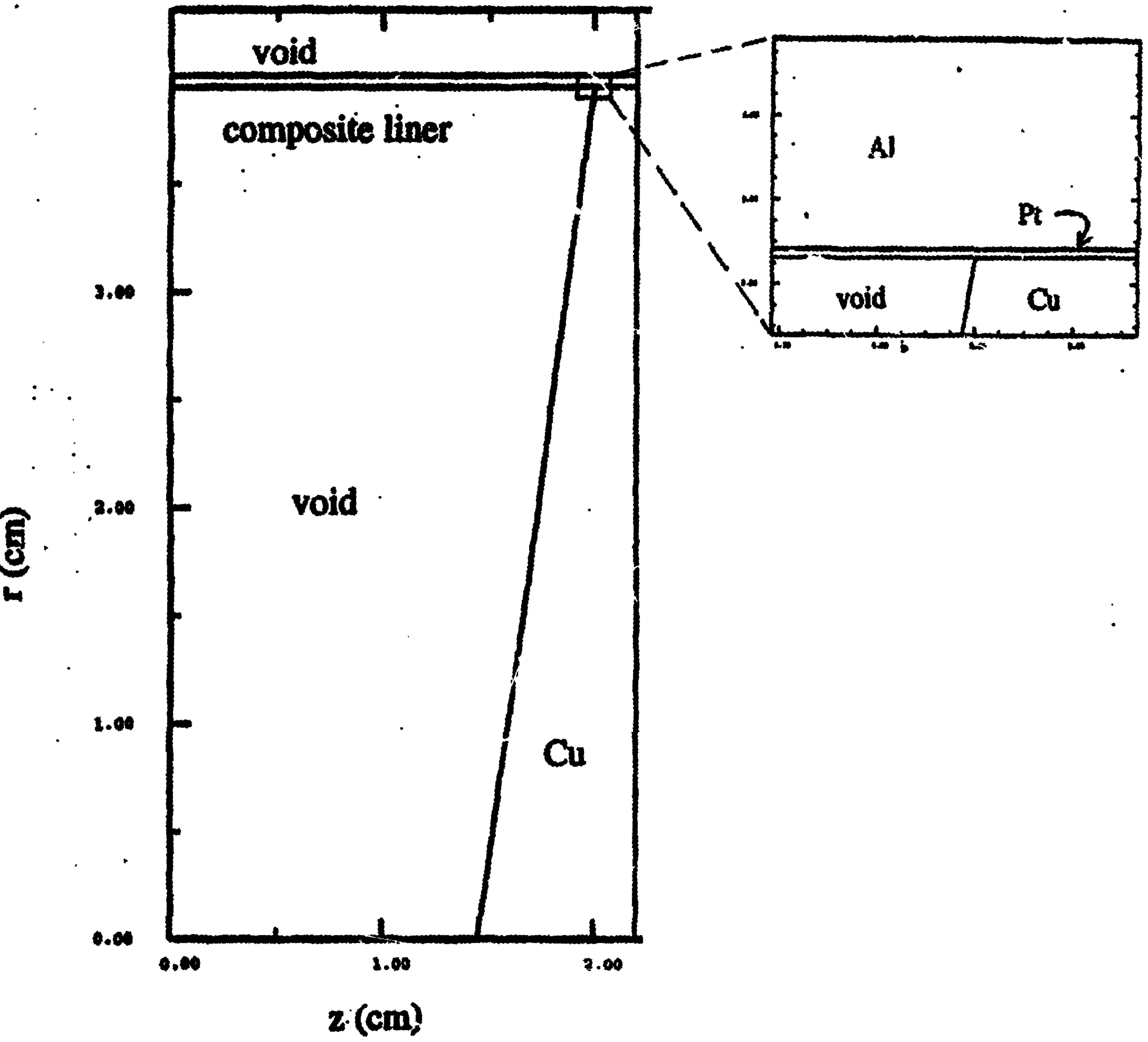
void
composite liner
void
Cu
3.00
2.00
1.00
0.00
r (cm)
0.00
1.00
2.00
z (cm)
Al
Pt
void
Cu

A-09 9.tif

Observations on the modified 2-D approach:

- 2-D models without a thin platinum layer over estimate the potential importance of instabilities
- stabilizing effects of plastically deforming aluminum permits inferences about stability with a thin platinum layer
- uncertainties in data bases, especially in melt and strength models, affect stability predictions
- data needed to benchmark code's ability to accurately describe evolution of instabilities in the liquid regime
- these calculations will serve a as possible benchmark for advanced methods (e.g., adaptive mesh refinement) which will be able to resolve thin layers.

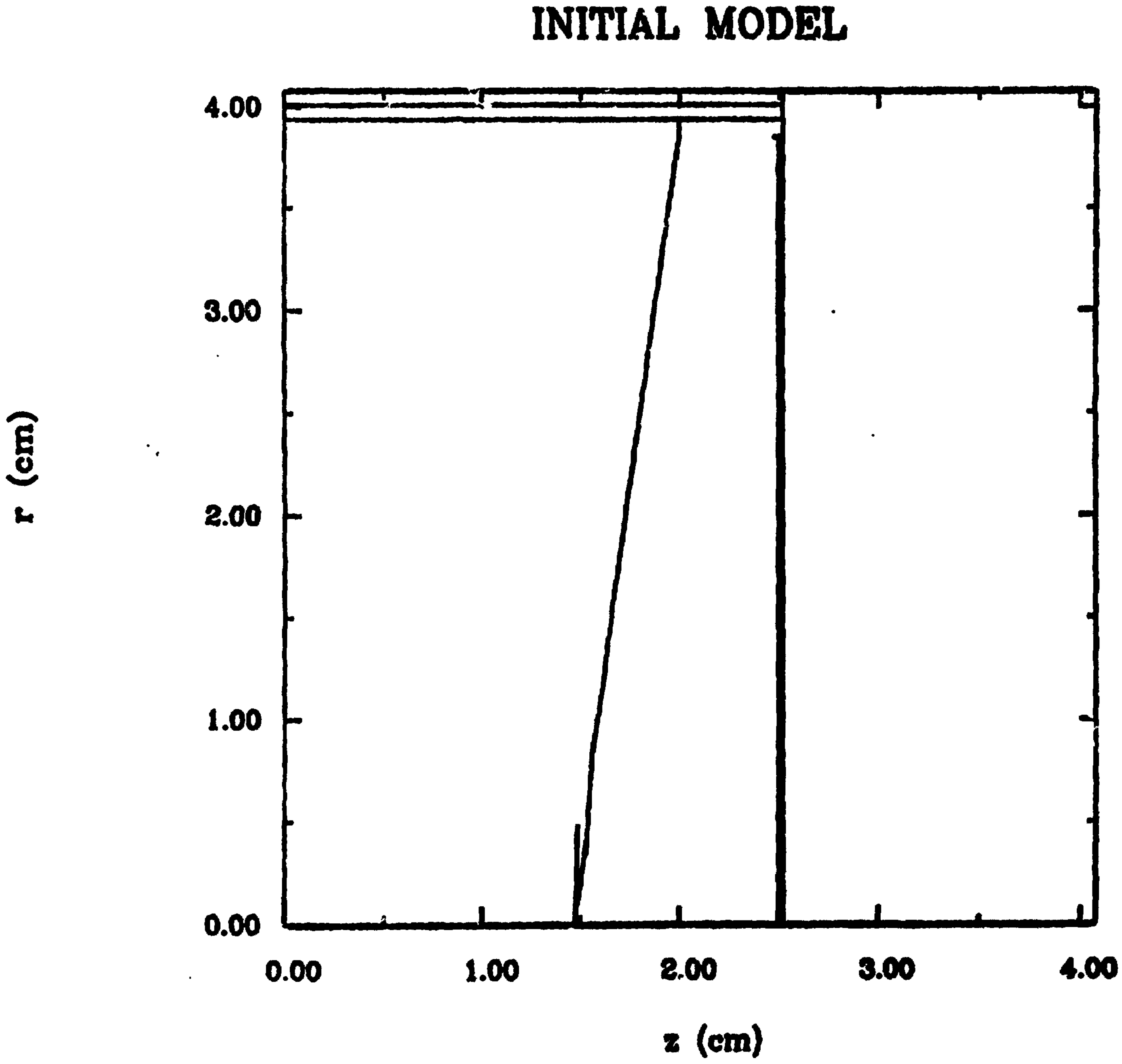
INITIAL MODEL
r (cm)
0.00
1.00
2.00
3.00
4.00
z (cm)
0.00
1.00
2.00
3.00
4.00

Designing the liner - electrode mounting

Contour plots of the equivalent plastic strain in the solid aluminum liner are shown at three times after the onset of current flow. Early time "beam bending" of the liner is minimal, and effective contact between the liner and the electrode is established. This design differs from that used in the solid liner-ejecta experiments.

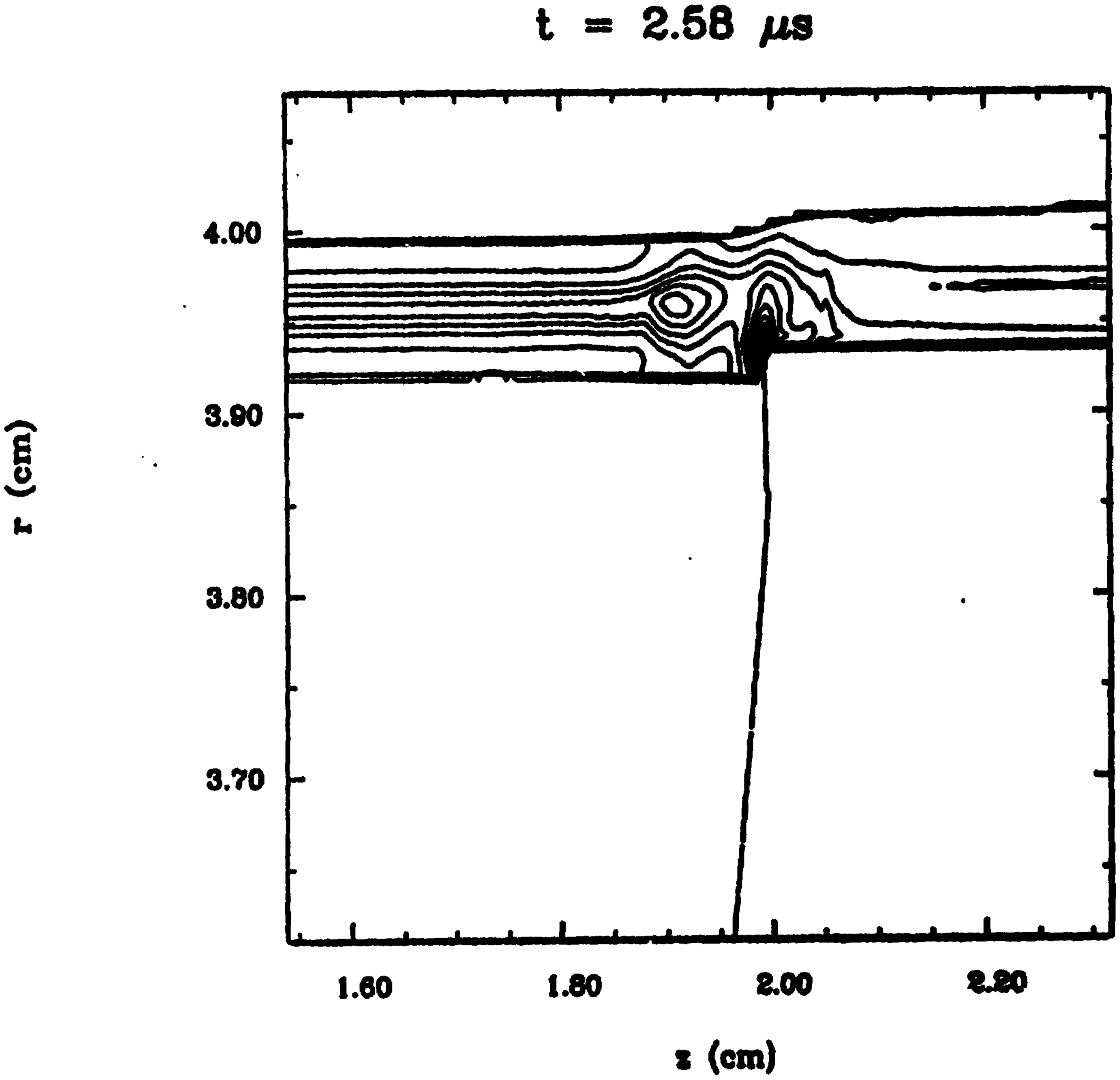
t = 2.58 μs
4.00
3.90
3.80
3.70
r (cm)
1.60
1.80
2.00
2.20
z (cm)

t = 3.53 μs

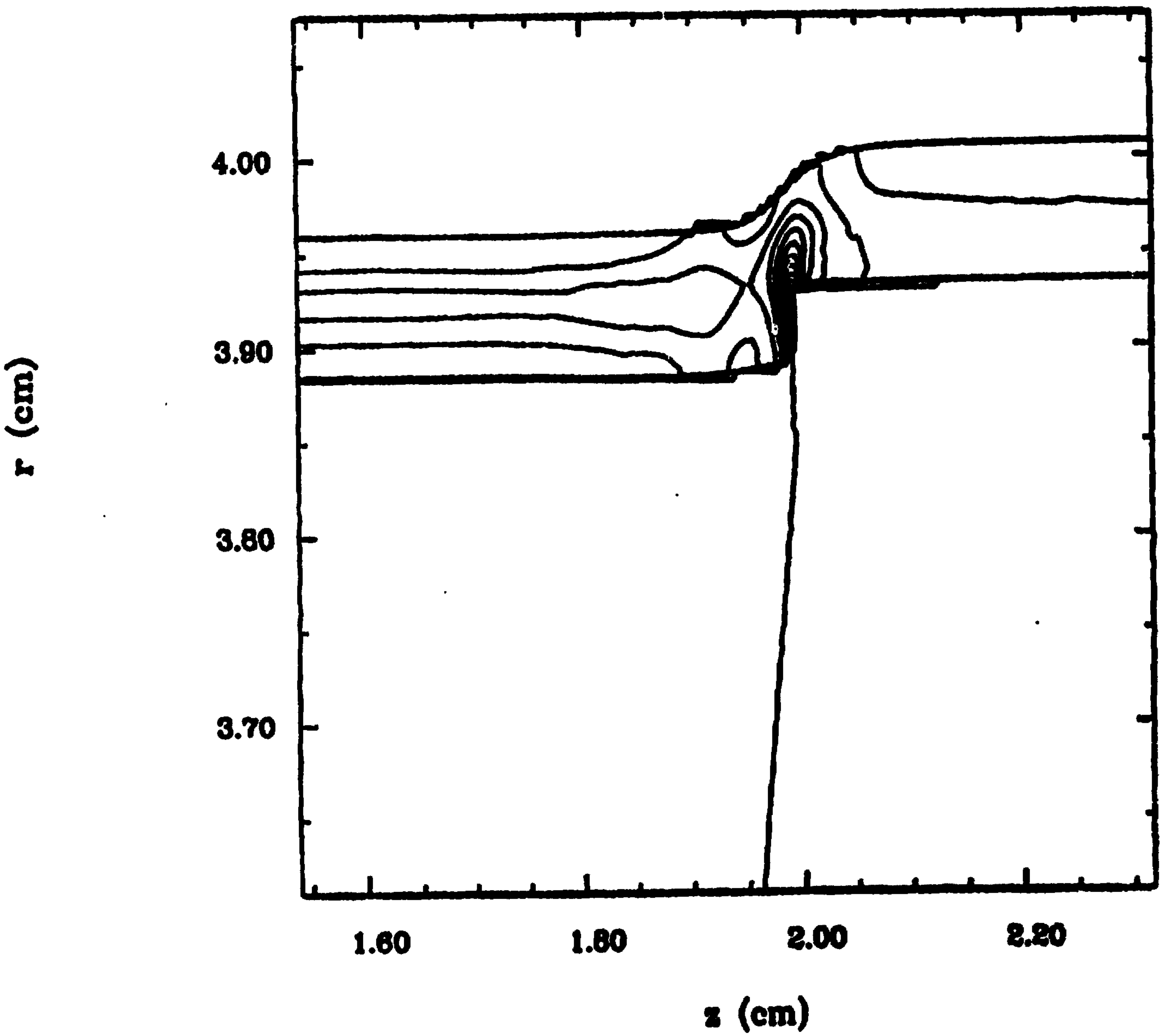

The implosion of a liner may involve four stages:

Stage 1: Initial deformation and launching of the liner

Initial elastic deformation, and onset of plastic flow
Establishes initial liner-electrode glide plane
First introduction of perturbations near the electrodes

Stage 2: Plastic deformation of liner

Liner plastically deforms as it implodes
Resistive heating and plastic heating occur in the liner and at the liner-electrode contacts
Perturbations induced as the liner moves along the electrodes

Stage 3: Onset of melt in the outer layers of the liner

Melt wave propagates from the outside of the liner toward the inside
Instability growth begins in liquid layer
Growth stops at the liquid-solid boundary
Inner solid layer continues inward plastic deformation

Stage 4: Platinum stabilized implosion to the target

Inner solid layer continues to heat (electrically and mechanically), while stabilizing overlying layer

Evolution of a pure aluminum, megabar liner driver; iso density contours of the liner and electrode in the r-z plane are shown for time 5 µs < t < 9.5 µs (note change in scale of the vertical axis)

---

t = 5 - 6 µs: Liner implodes plastically, maintaining contact with the electrode. During this stage the entire liner remains solid. Small perturbations arise near the electrode.

t = 6.56 µs: The backside of the liner begins to melt, and a melt wave moves inward.

t = 7 µs: The melt wave has passed about half way through the liner. Perturbations in the overlying liquid layer begin to grow.

t = 8 µs: The inner layer of aluminum remains solid away from the electrode. Melt reaches the inner surface near the electrode. Instability growth in the liquid layer has become significant near the electrode, but is limited by the underlying solid layer.

t = 8.5 µs: Melt reaches a significant portion of the inner surface near the electrode. Instability growth resumes.

t = 9 - 9.5 µs: Once the entire aluminum layer has melted instabilities grow, disrupting the liner near the electrode. Low density plasma and magnetic field are accelerated ahead of the liner as "bubbles" pop.

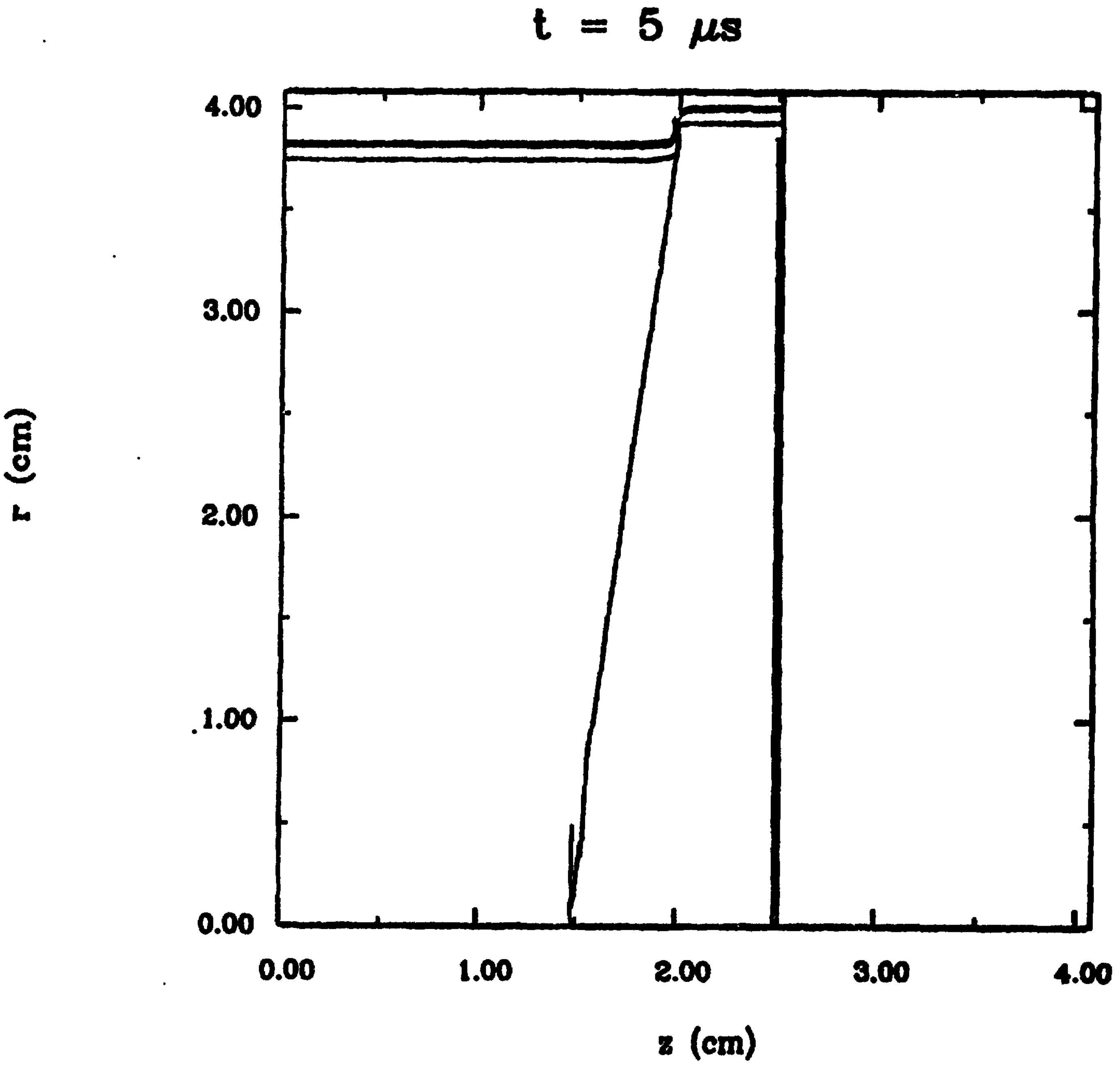
t = 5 μs
4.00
3.00
2.00
1.00
0.00
r (cm)
0.00
1.00
2.00
3.00
4.00
z (cm)

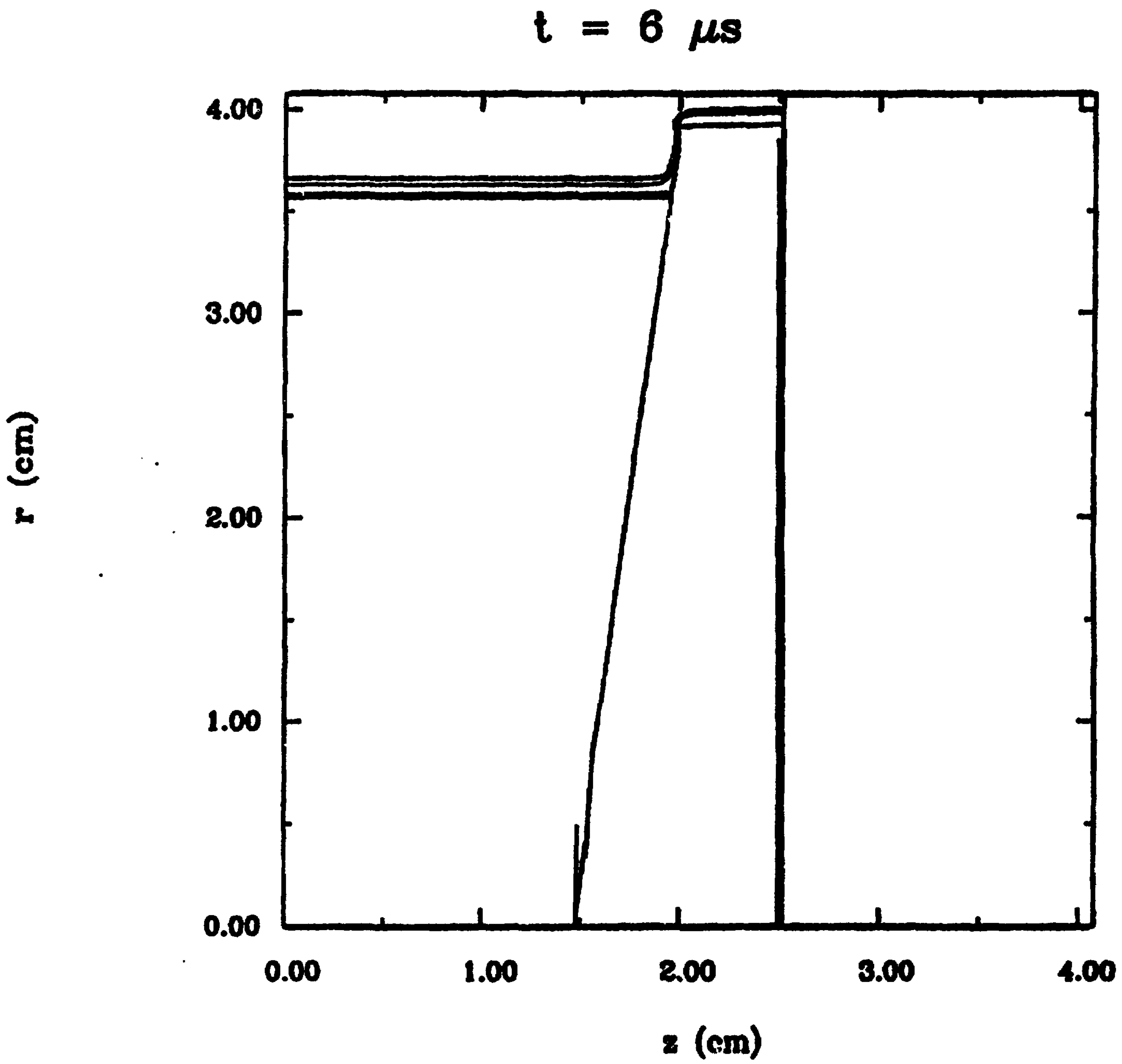

t = 6 μs

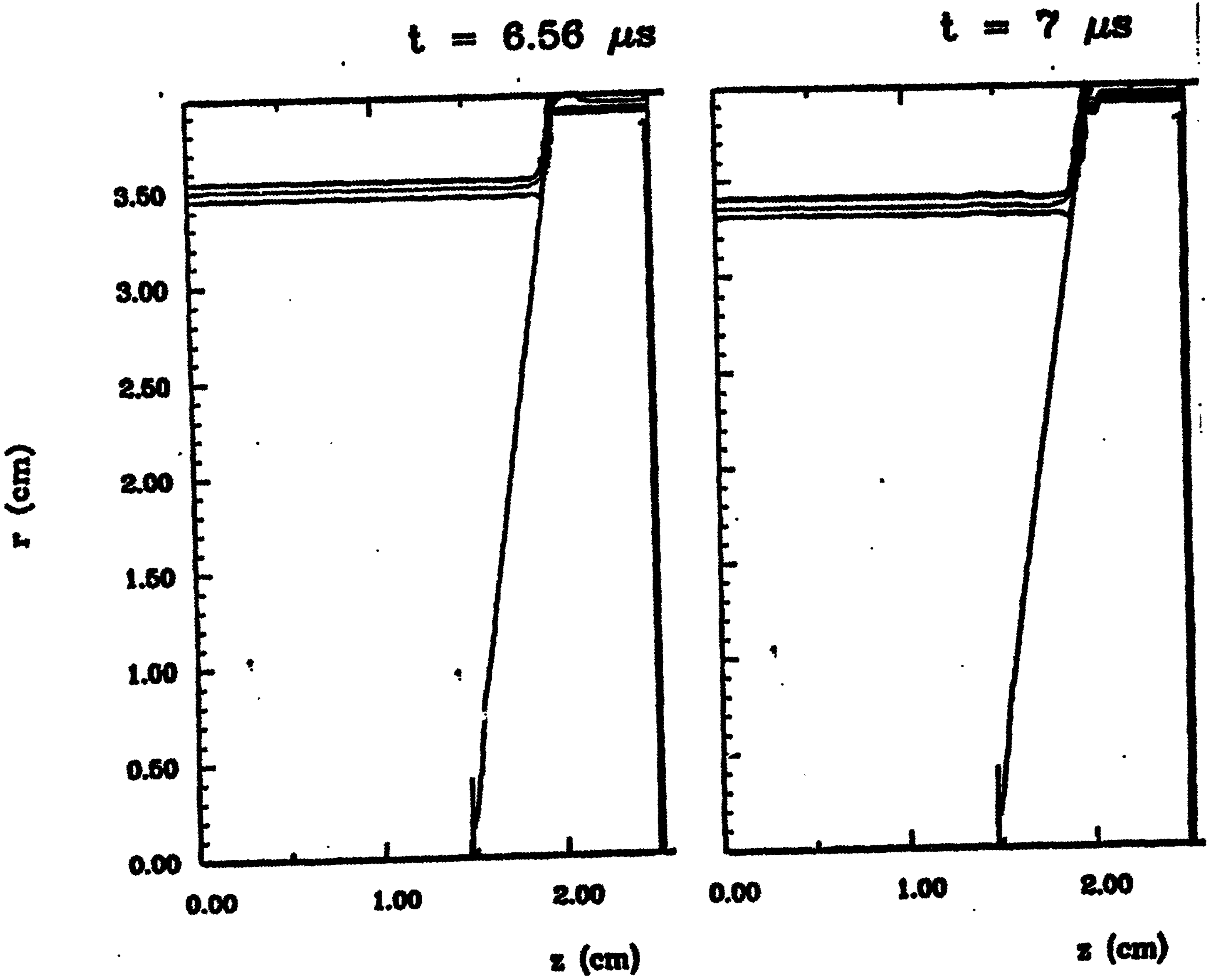
t = 6.56 μs
t = 7 μs
r (cm)
3.50
3.00
2.50
2.00
1.50
1.00
0.50
0.00
0.00
1.00
2.00
z (cm)
0.00
1.00
2.00
z (cm)

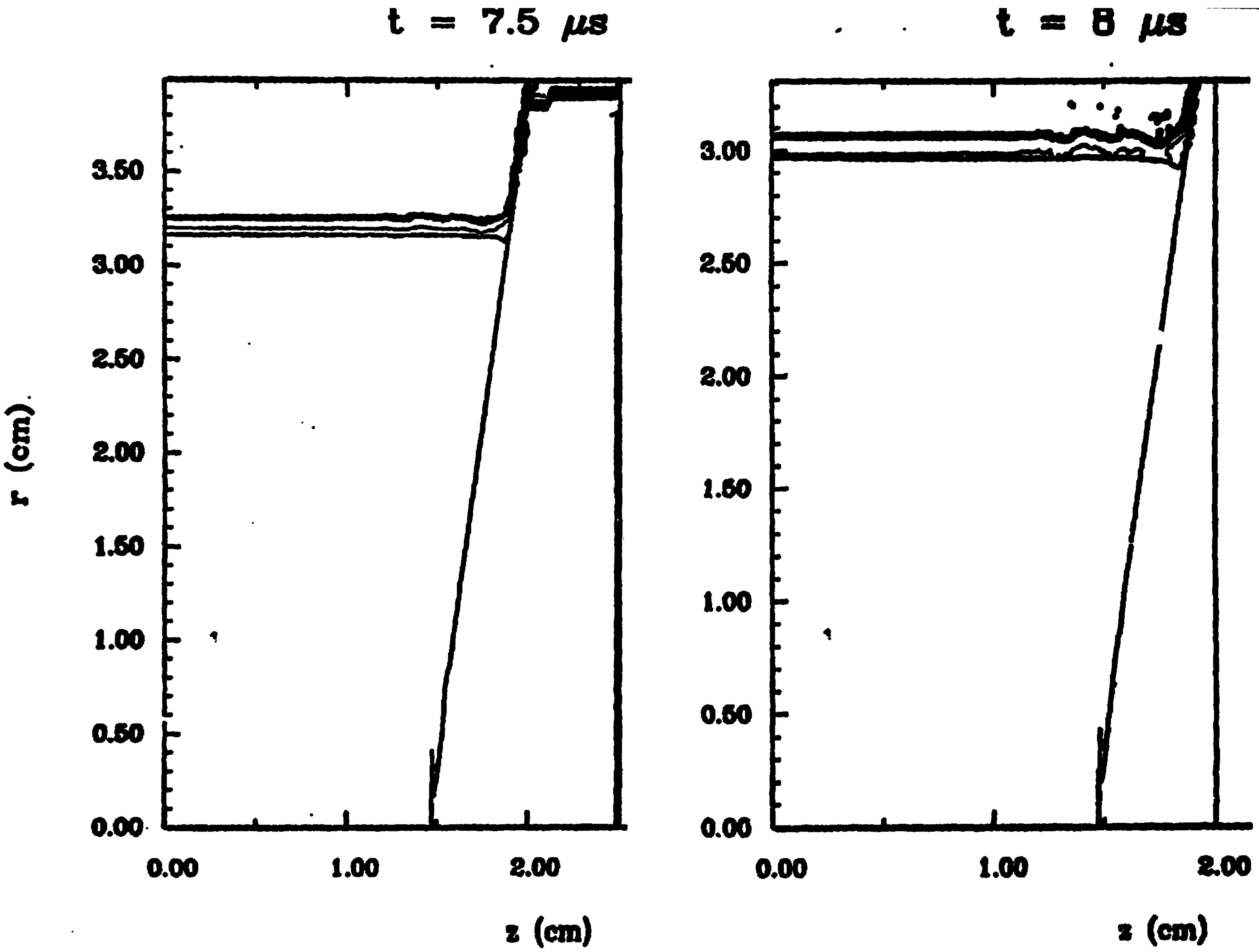
t = 7.5 μs
t = 8 μs
r (cm)
3.50
3.00
2.50
2.00
1.50
1.00
0.50
0.00
0.00
1.00
2.00
z (cm)
3.00
2.50
2.00
1.50
1.00
0.50
0.00
0.00
1.00
2.00
z (cm)

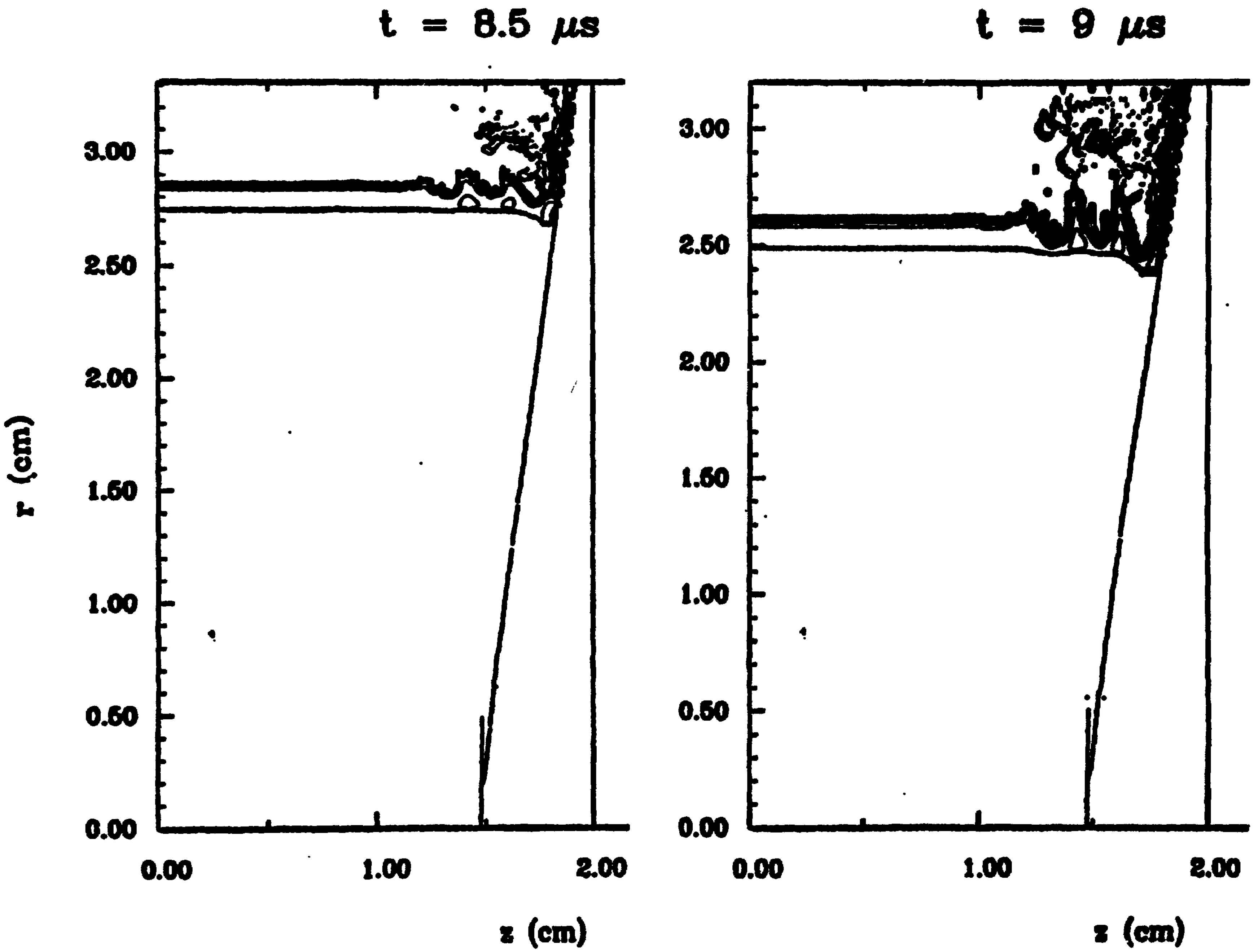
t = 8.5 μs
t = 9 μs
r (cm)
3.00
2.50
2.00
1.50
1.00
0.50
0.00
0.00
1.00
2.00
z (cm)
3.00
2.50
2.00
1.50
1.00
0.50
0.00
0.00
1.00
2.00
z (cm)

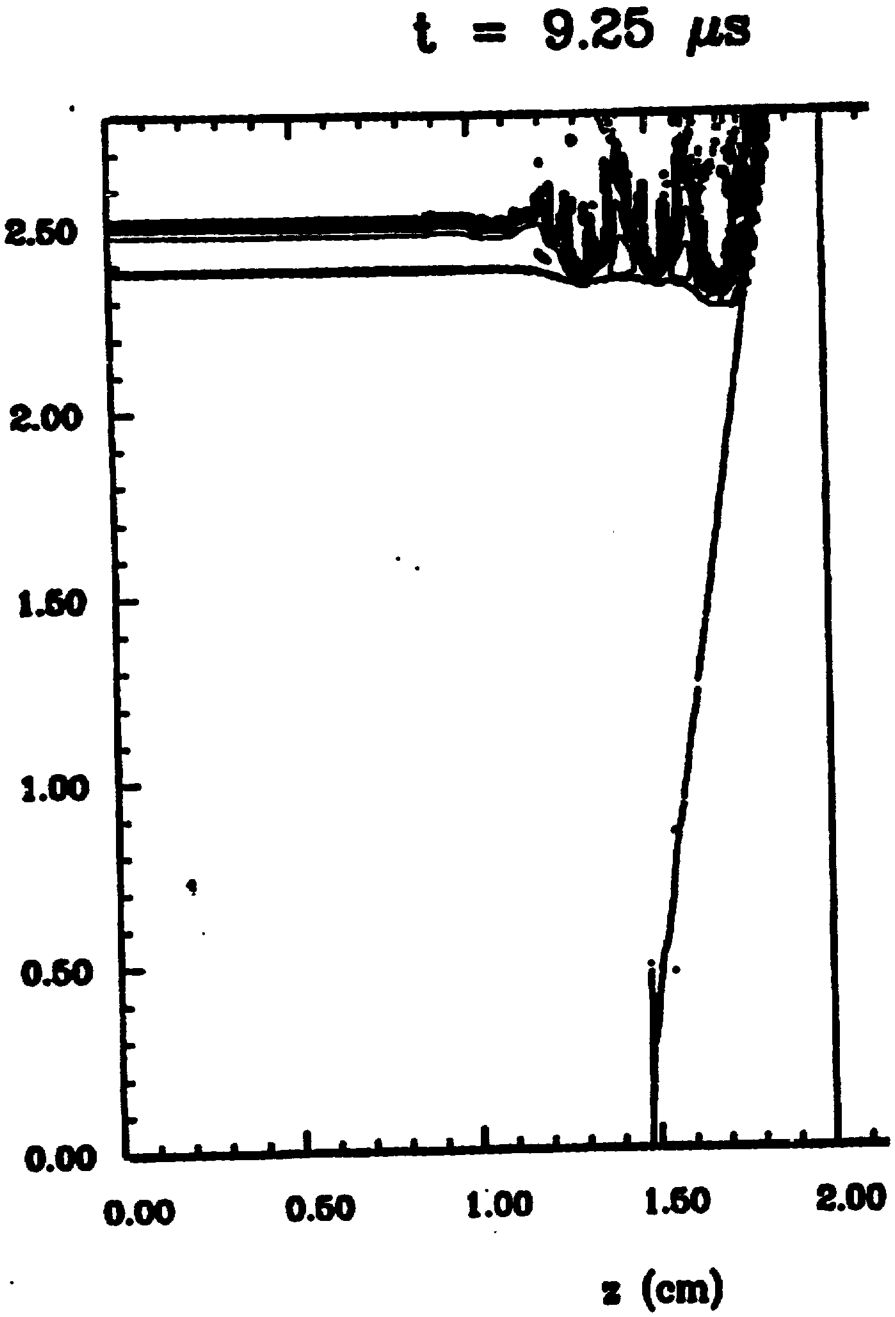

t = 9.25 μs

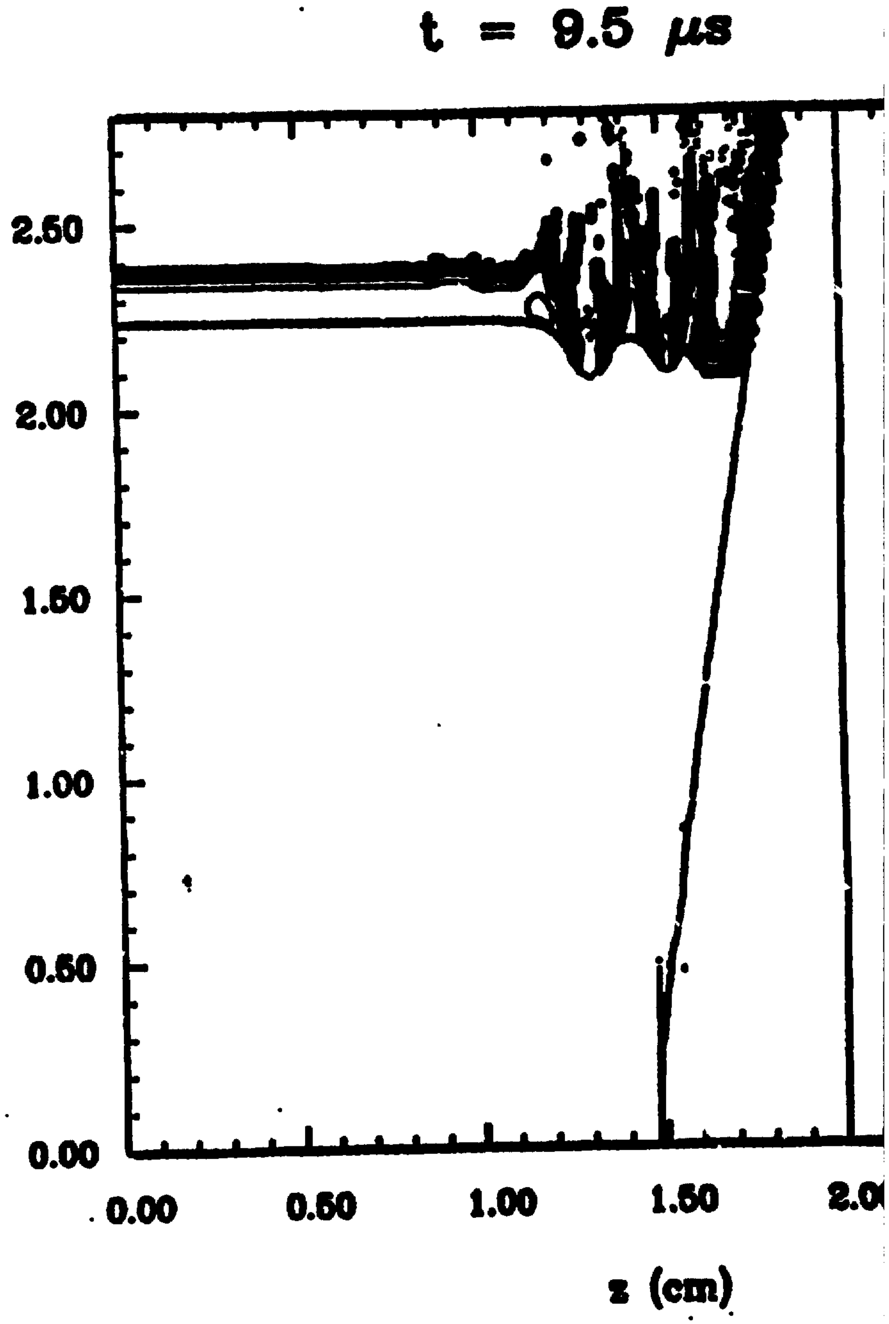

t = 9.5 μs

Evolution of the melt region in the pure aluminum liner

Contours of the material strength stress tensor (radial component) are shown in the r - z plane. The stress tensor vanishes in portions of the liner that have melted (regions containing no contours).

t = 6.45 μs: portions of the liner away from the electrodes are solid, but the aluminum has started to melt near the electrode. Note the perturbation near z = 1.75 cm, and smaller ones at z = 1.55 cm and z = 1.3 cm;

t = 6.5 μs: melt starts at the outside surface of the liner;

t = 6.7 μs: dispite instability growth on the outside surface, the inner surface is still smooth;

t = 7 - 7.5 μs: instability growth is limited in amplitude to a fraction of the radial thickness of the liquid layer;

t = 7.9 μs: melt reaches the inner surface of the liner nearest the electrode;

t = 8.5 μs: melt of the aluminum liner is essentially complete, and instabilities now grow rapidly;

t = 6.45 μs

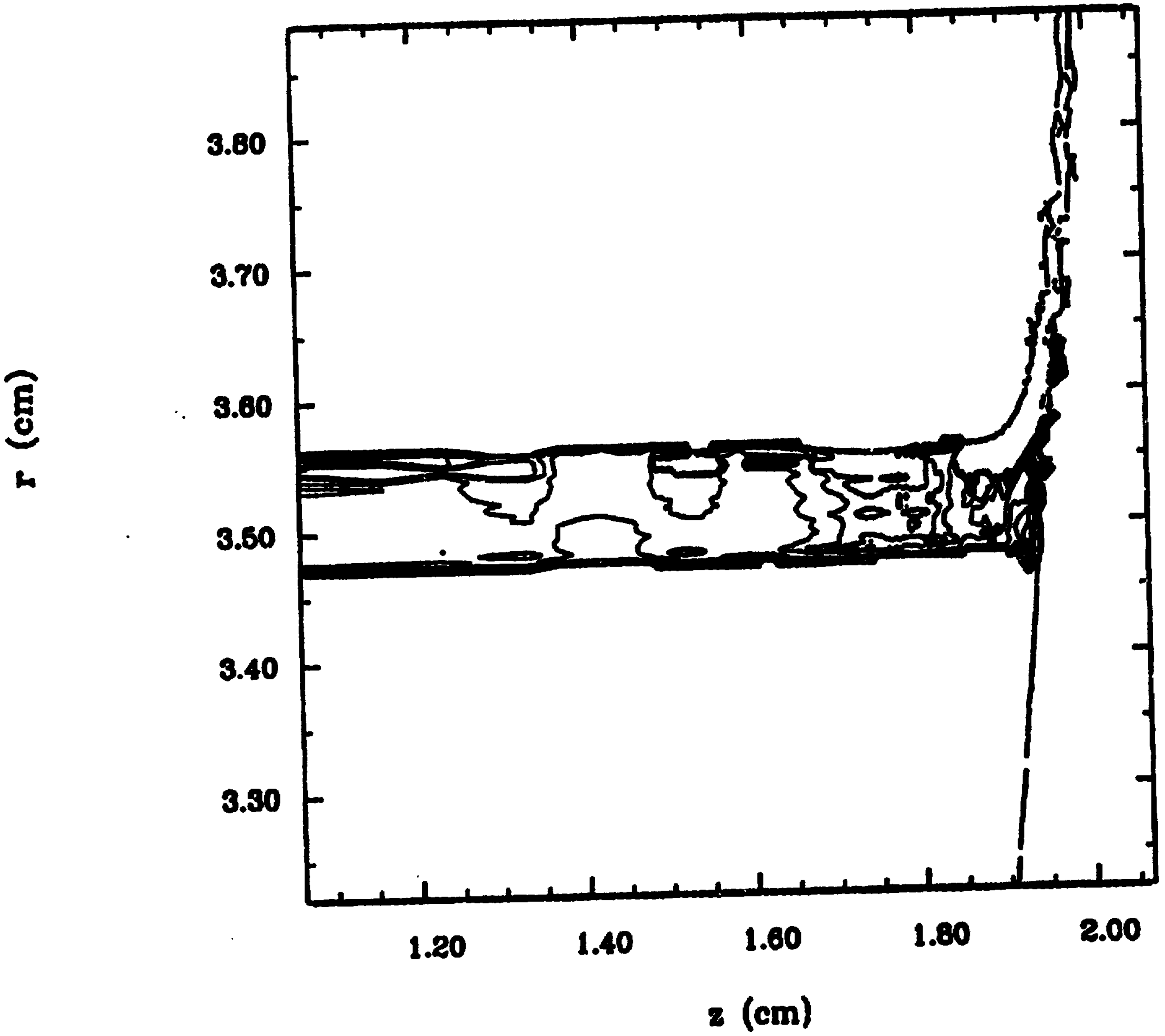

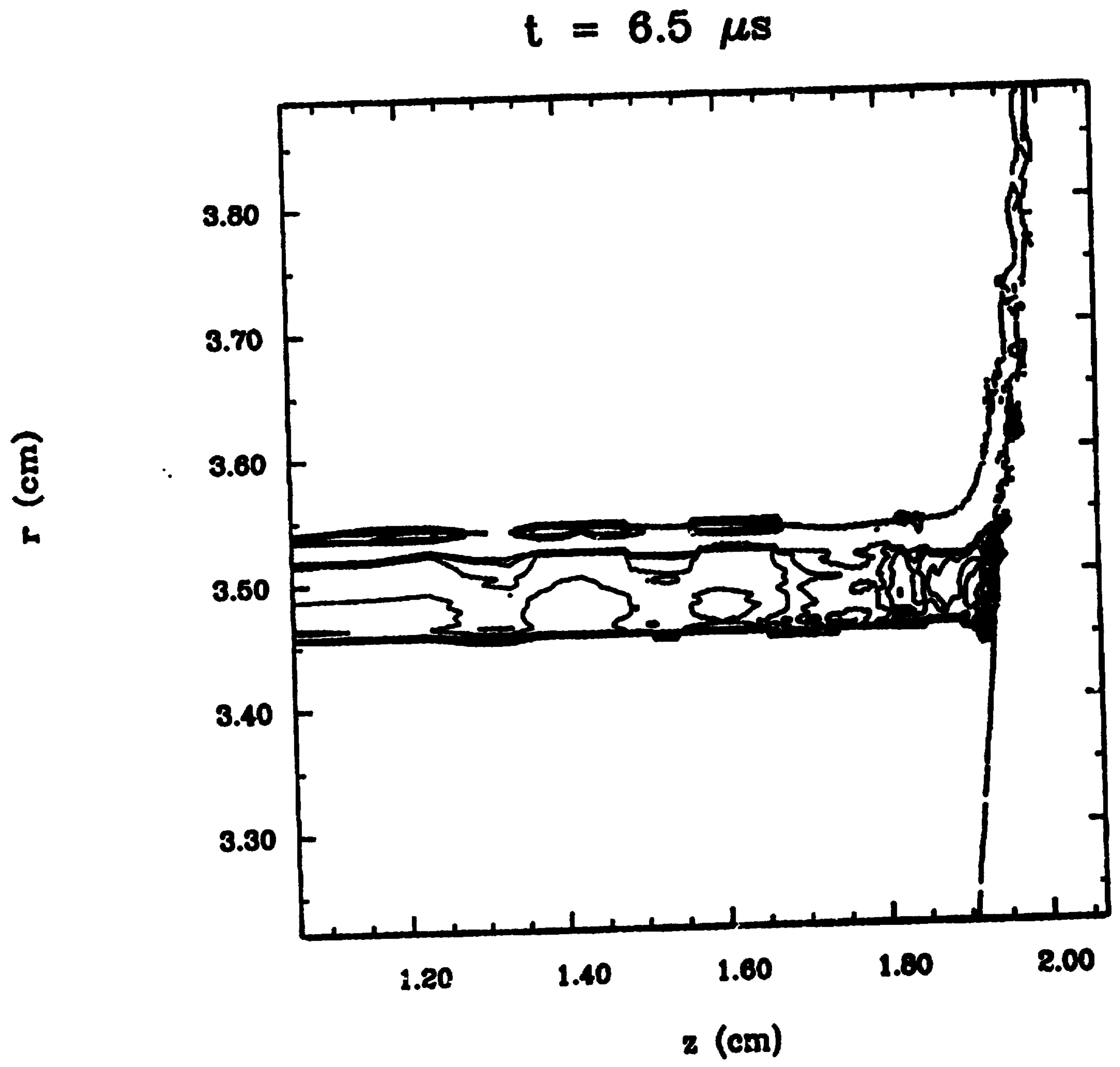
t = 6.5 μs
3.80
3.70
3.60
3.50
3.40
3.30
r (cm)
1.20
1.40
1.60
1.80
2.00
z (cm)

t = 6.7 μs

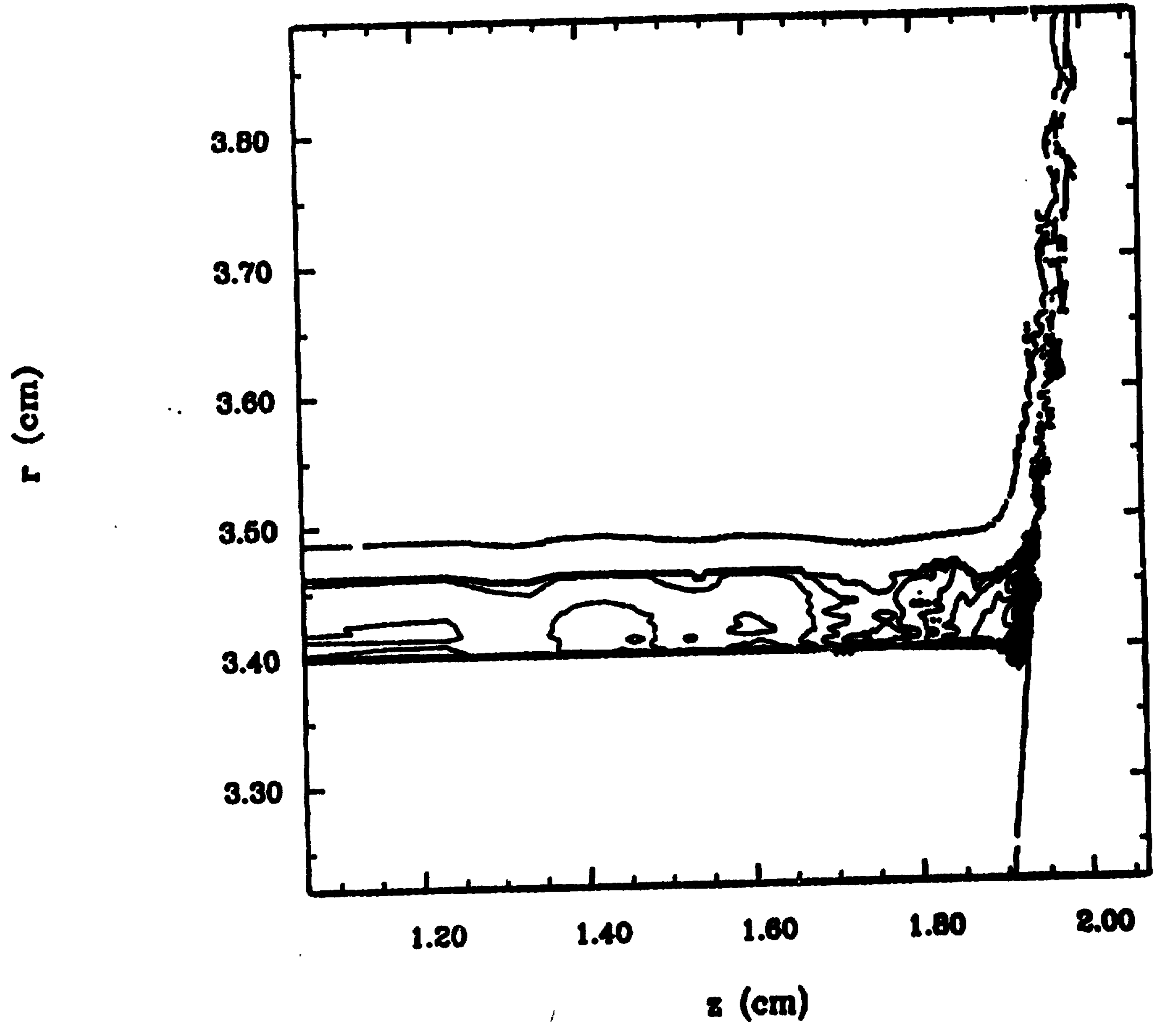

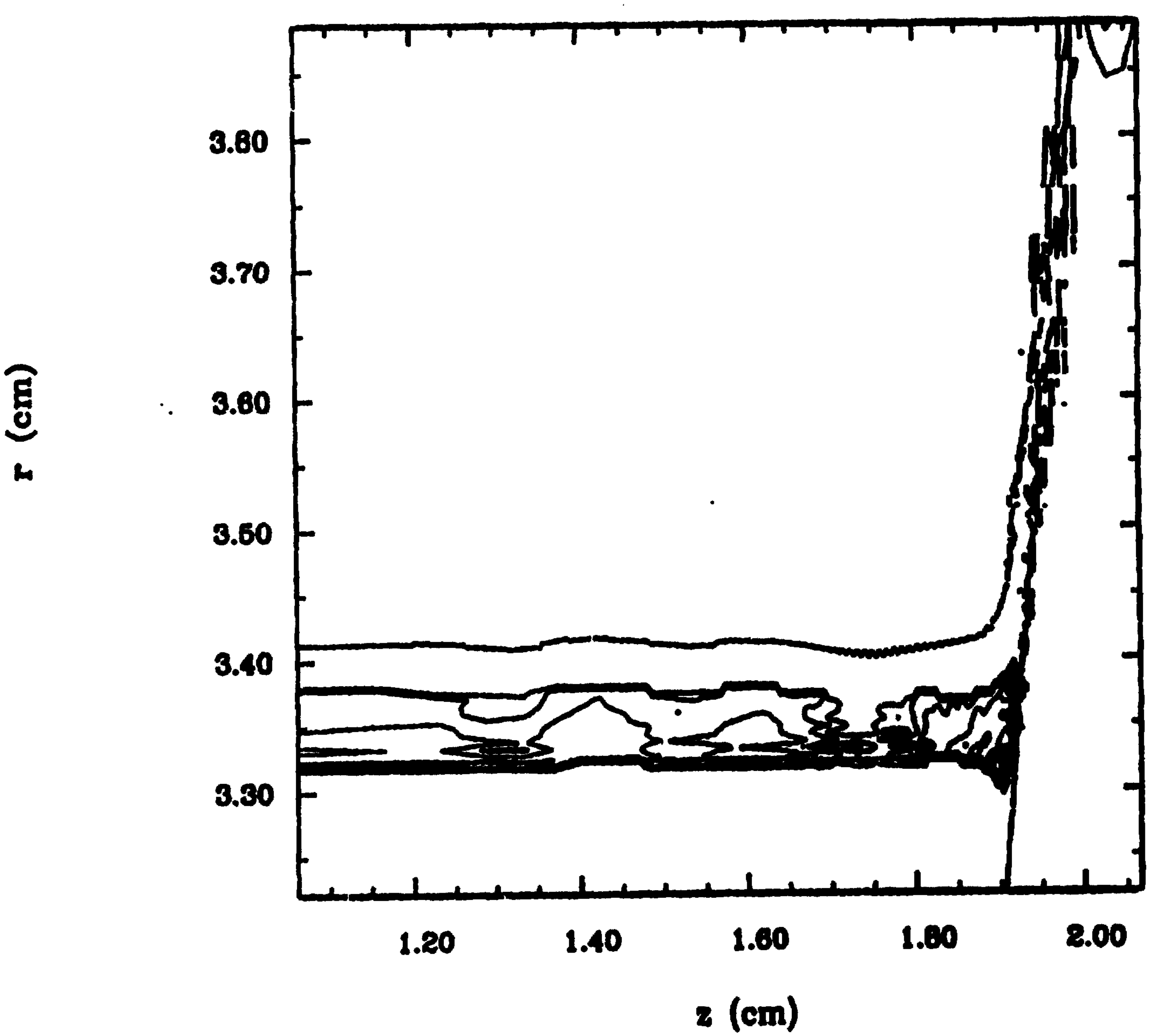

t = 7 μs

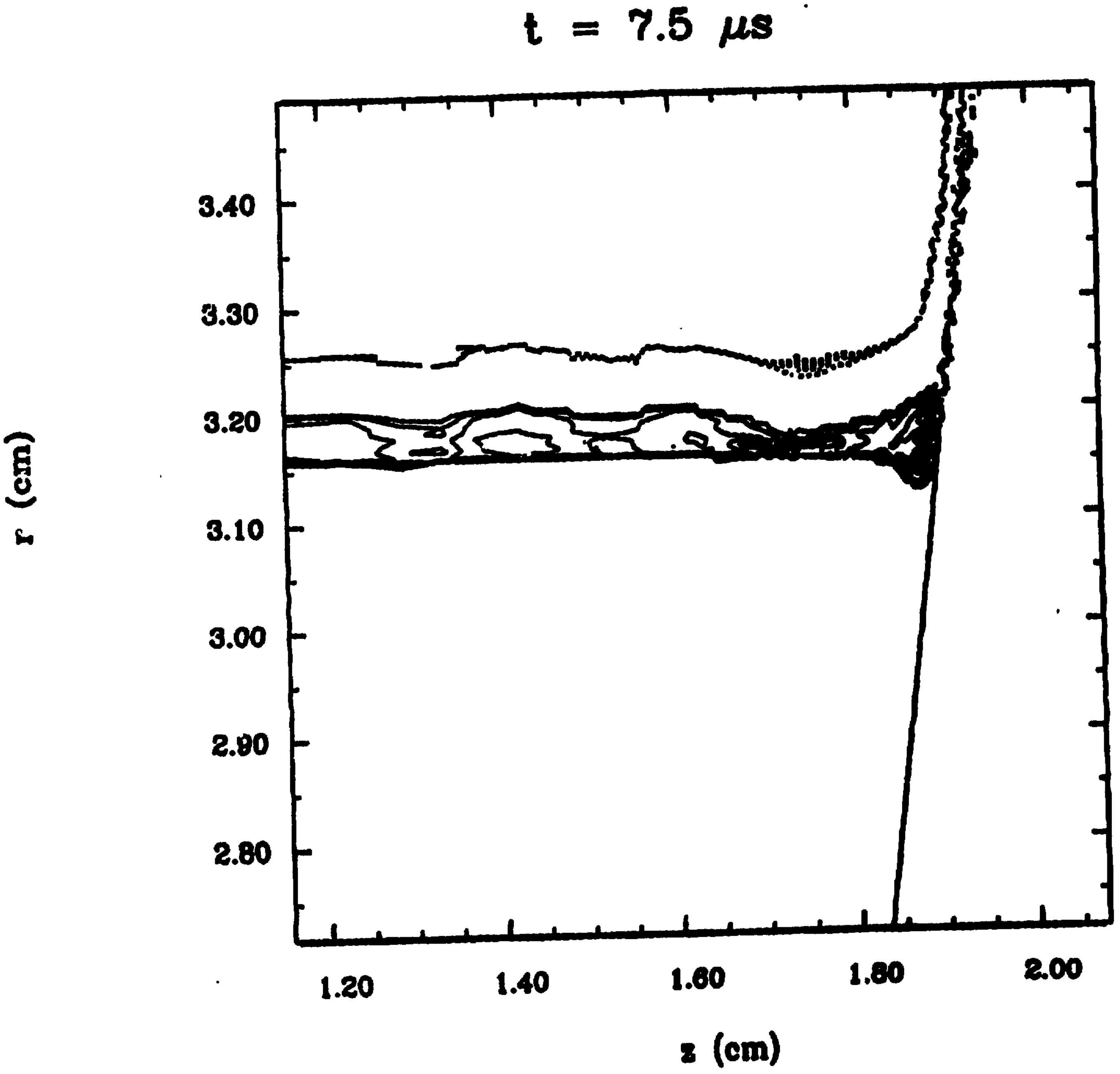
t = 7.5 μs
3.40
3.30
3.20
3.10
3.00
2.90
2.80
r (cm)
1.20
1.40
1.60
1.80
2.00
z (cm)

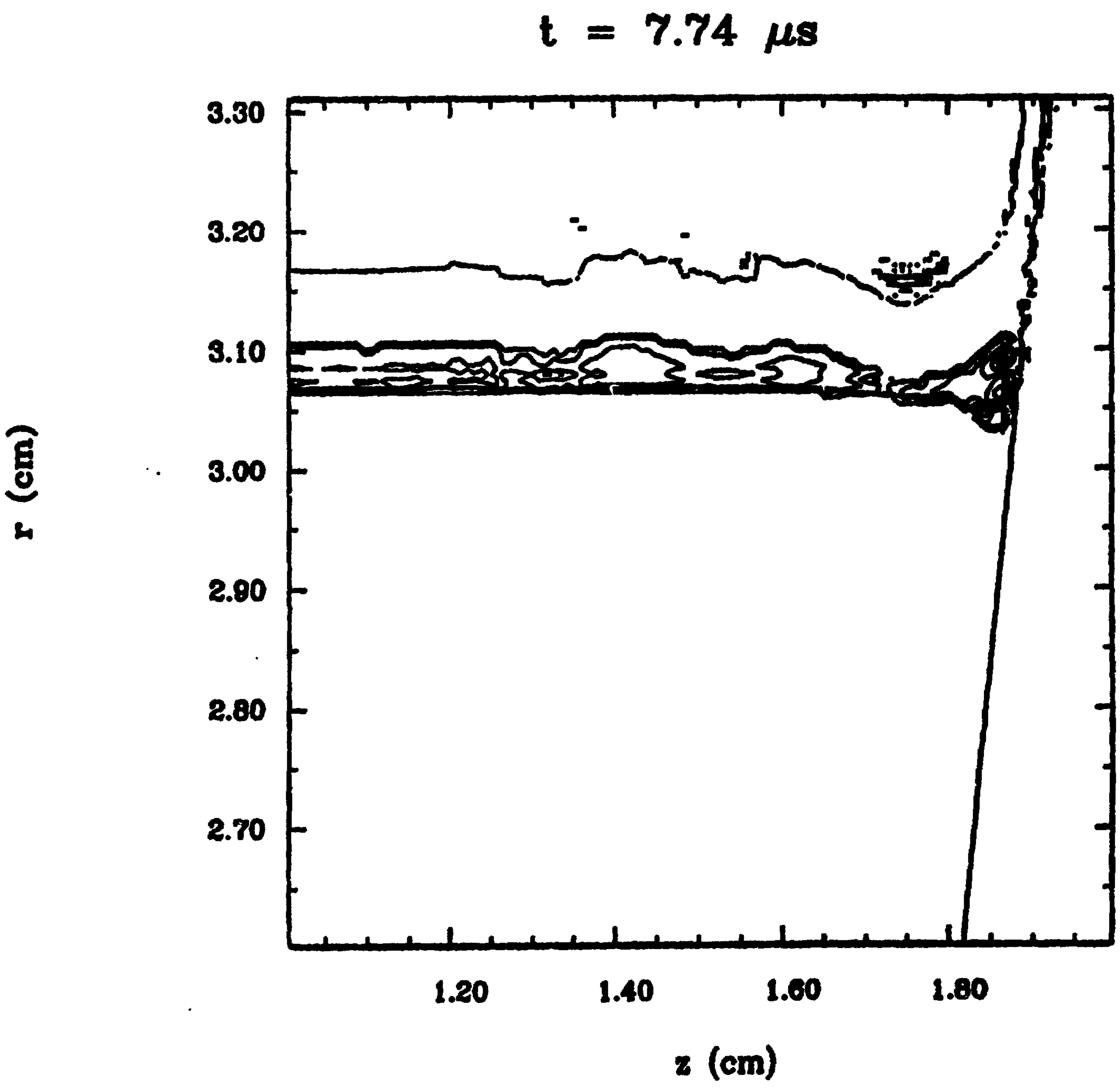
t = 7.74 μs
3.30
3.20
3.10
3.00
2.90
2.80
2.70
r (cm)
1.20
1.40
1.60
1.80
z (cm)

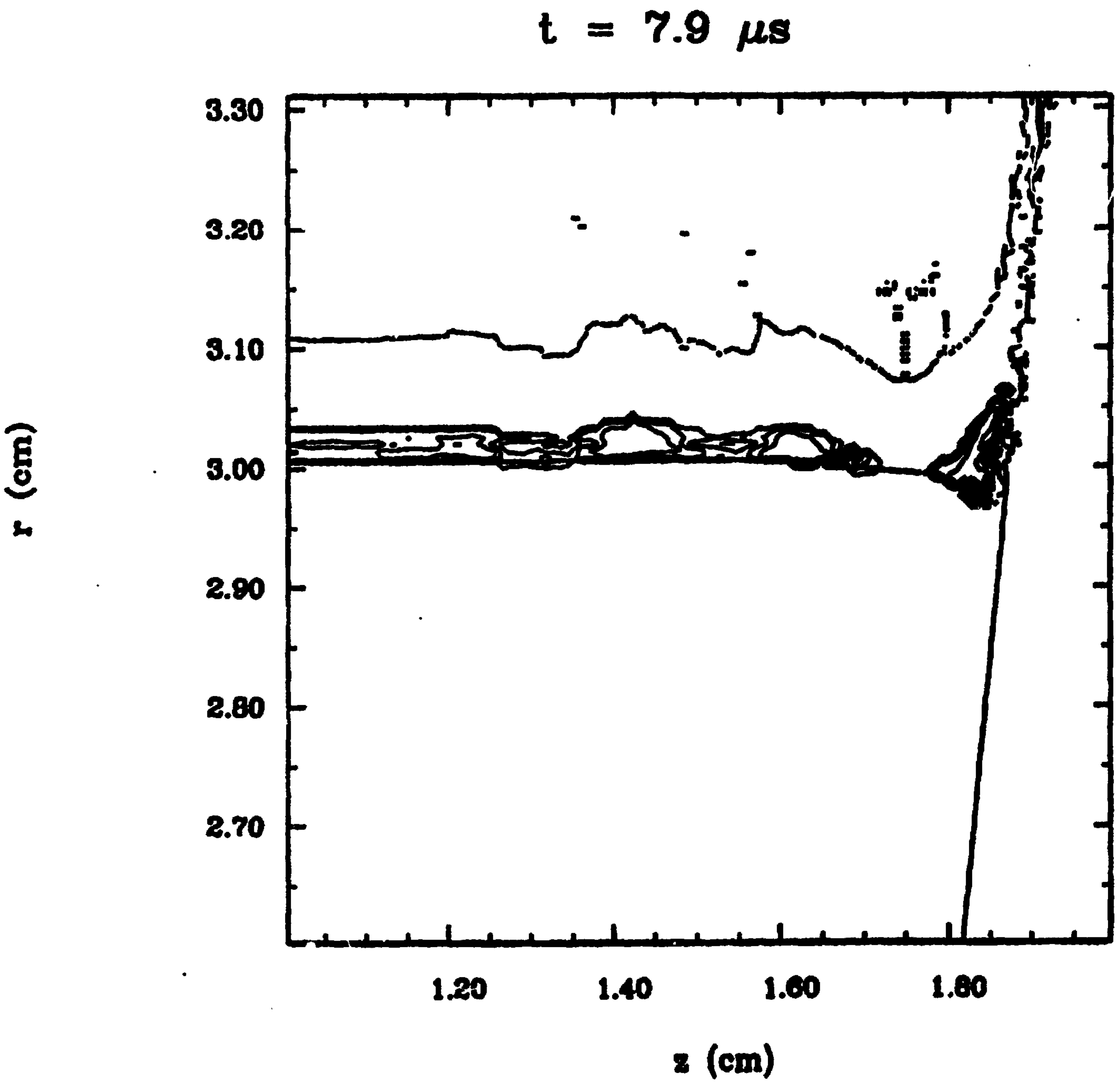
t = 7.9 μs
r (cm)
3.30
3.20
3.10
3.00
2.90
2.80
2.70
1.20
1.40
1.60
1.80
z (cm)

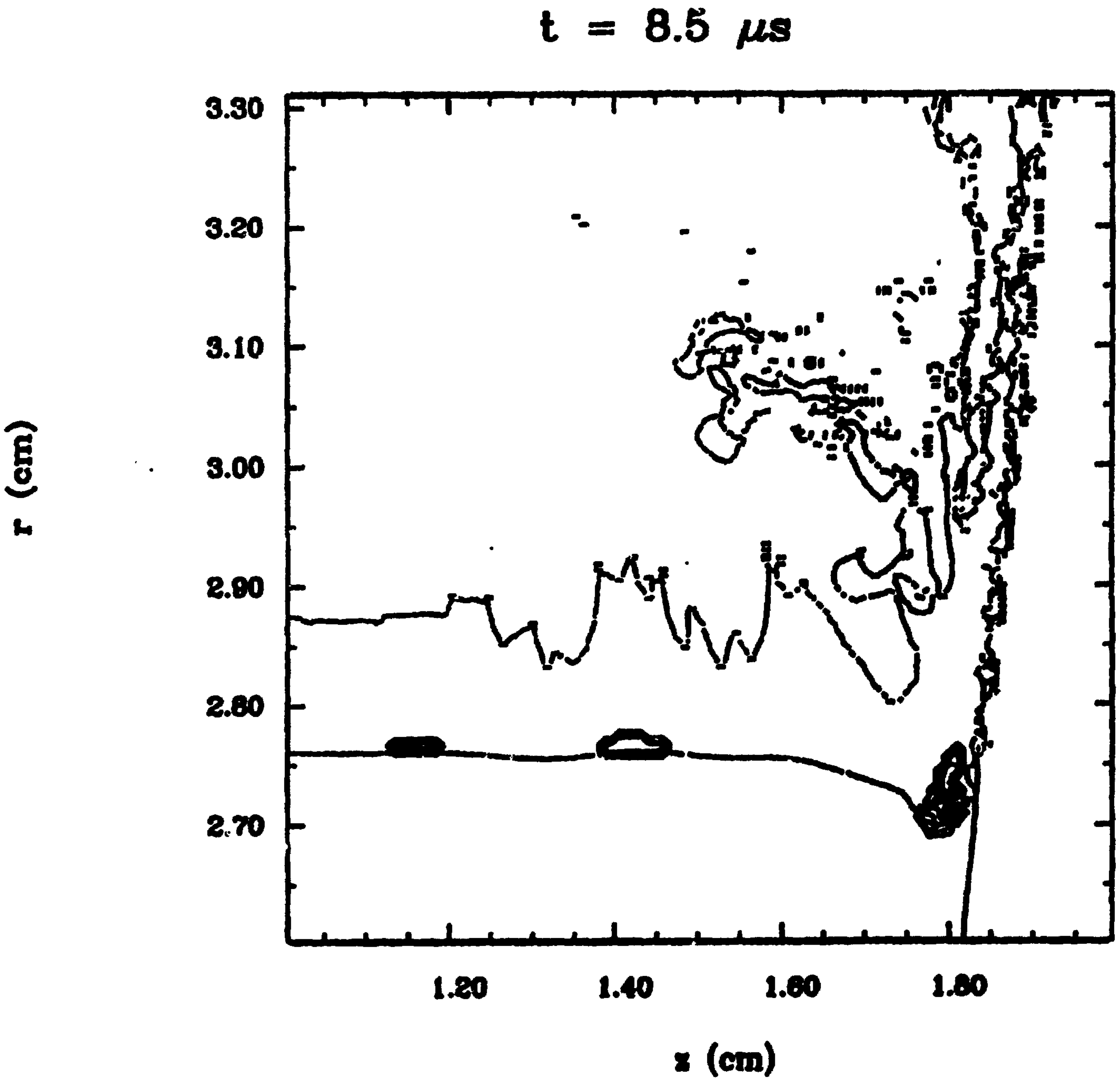
t = 8.5 μs
3.30
3.20
3.10
3.00
2.90
2.80
2.70
r (cm)
1.20
1.40
1.60
1.80
z (cm)

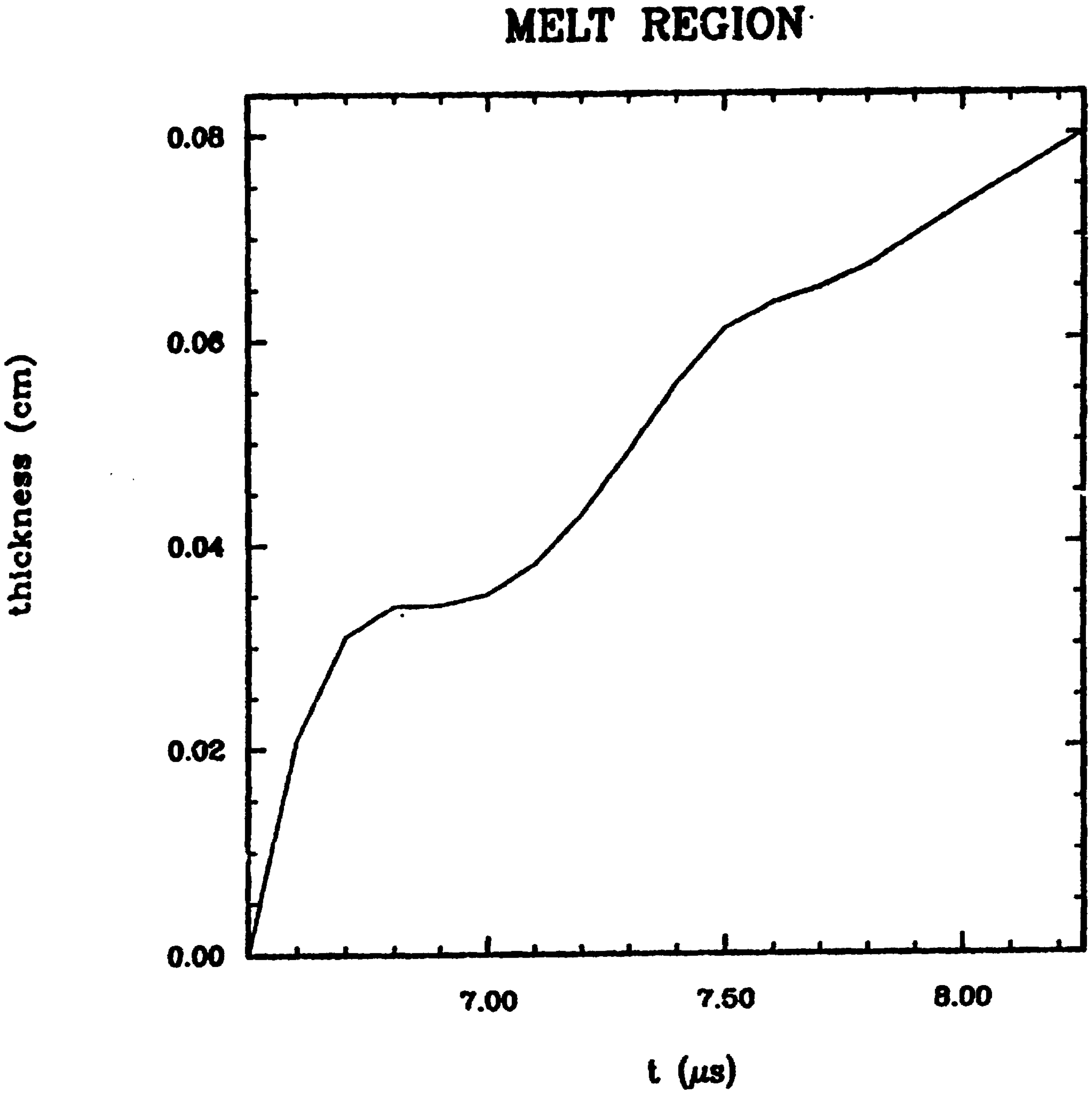
MELT REGION
thickness (cm)
0.00
0.02
0.04
0.06
0.08
7.00
7.50
8.00
t (μs)

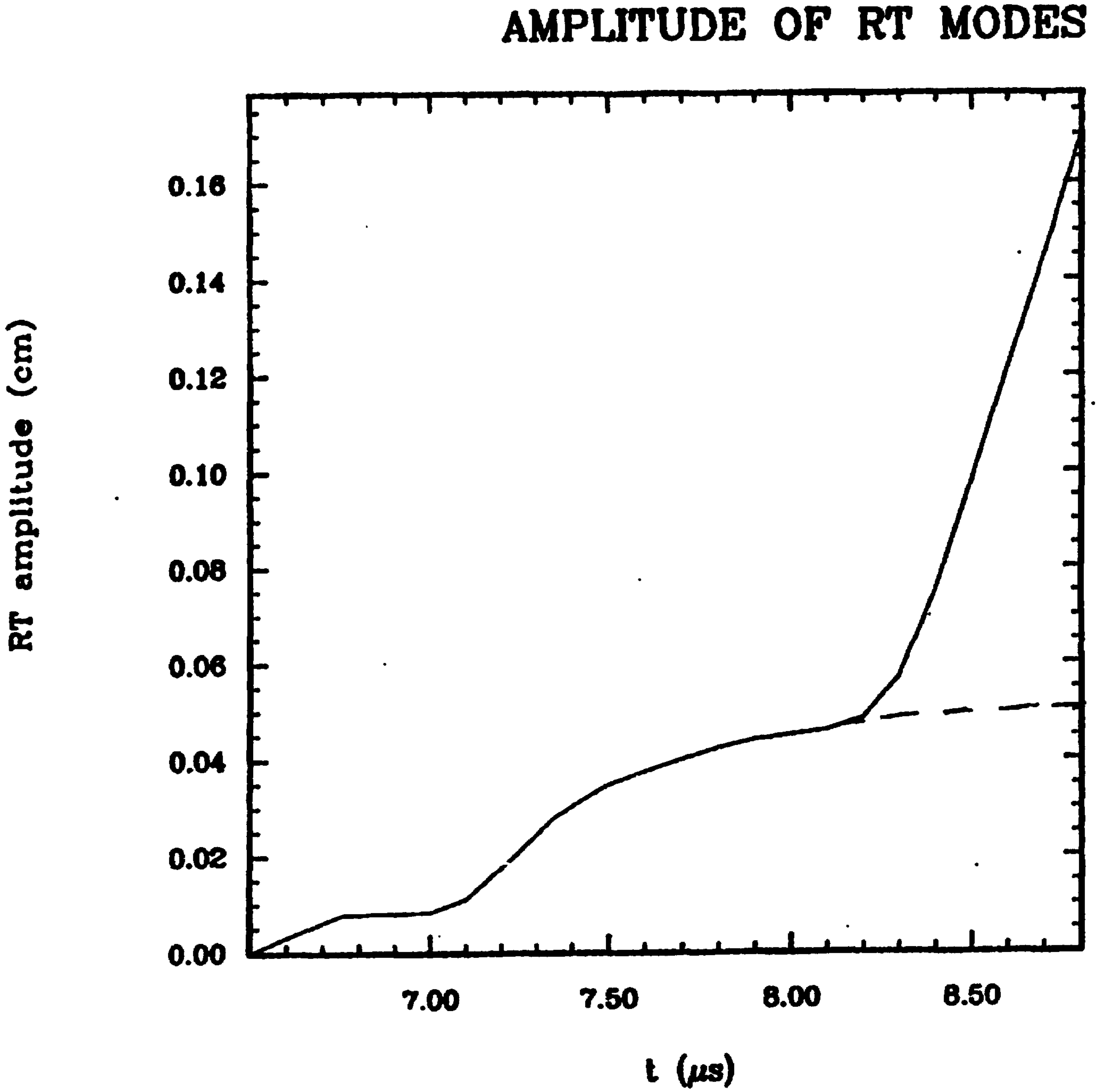
AMPLITUDE OF RT MODES
RT amplitude (cm)
0.00
0.02
0.04
0.06
0.08
0.10
0.12
0.14
0.16
7.00
7.50
8.00
8.50
t (μs)

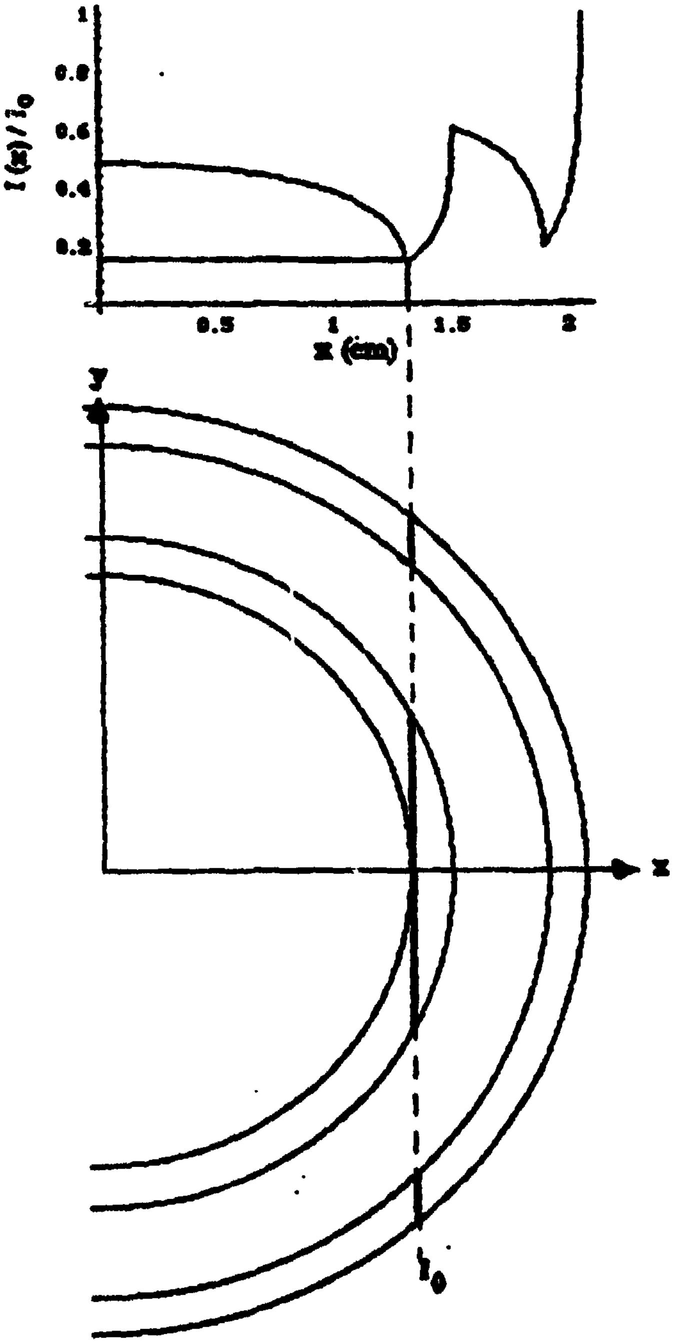

Figure 4. Line Scan Interpretation

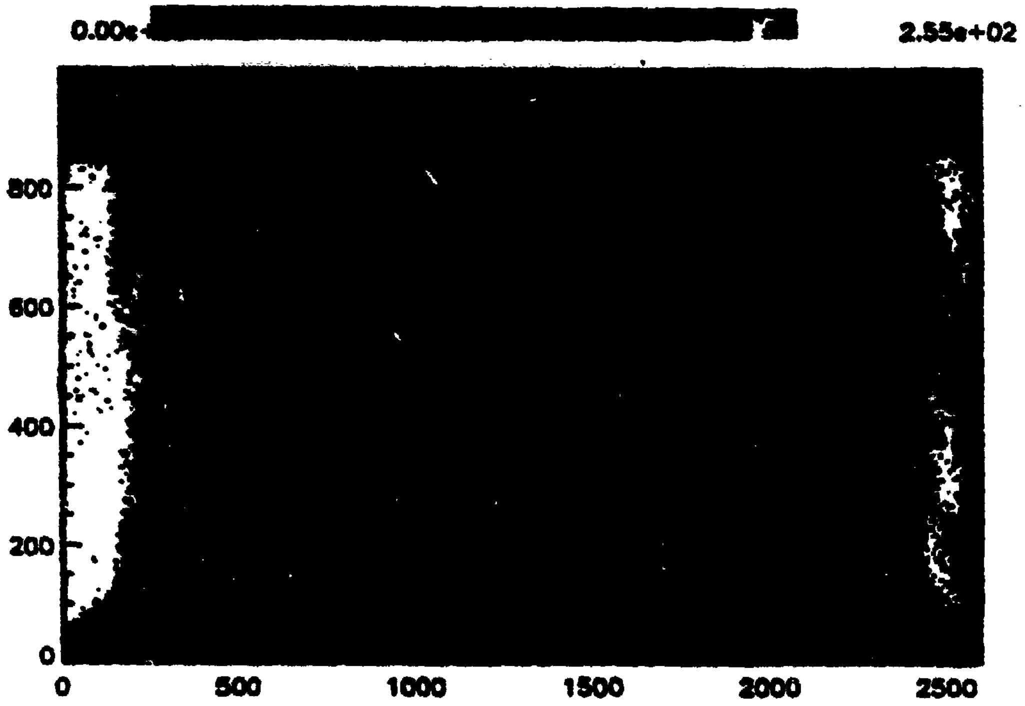

Figure 2. Megabar 1 Radiometry image

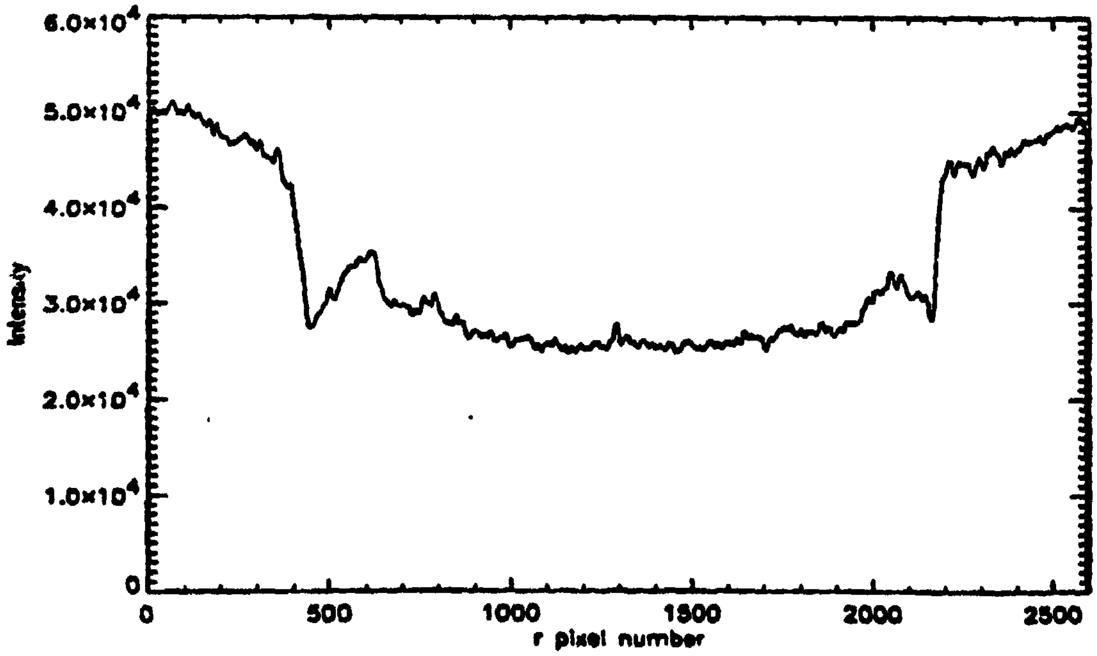

Figure 3. Line Scan (line 780) from Figure 2 in Radial Direction

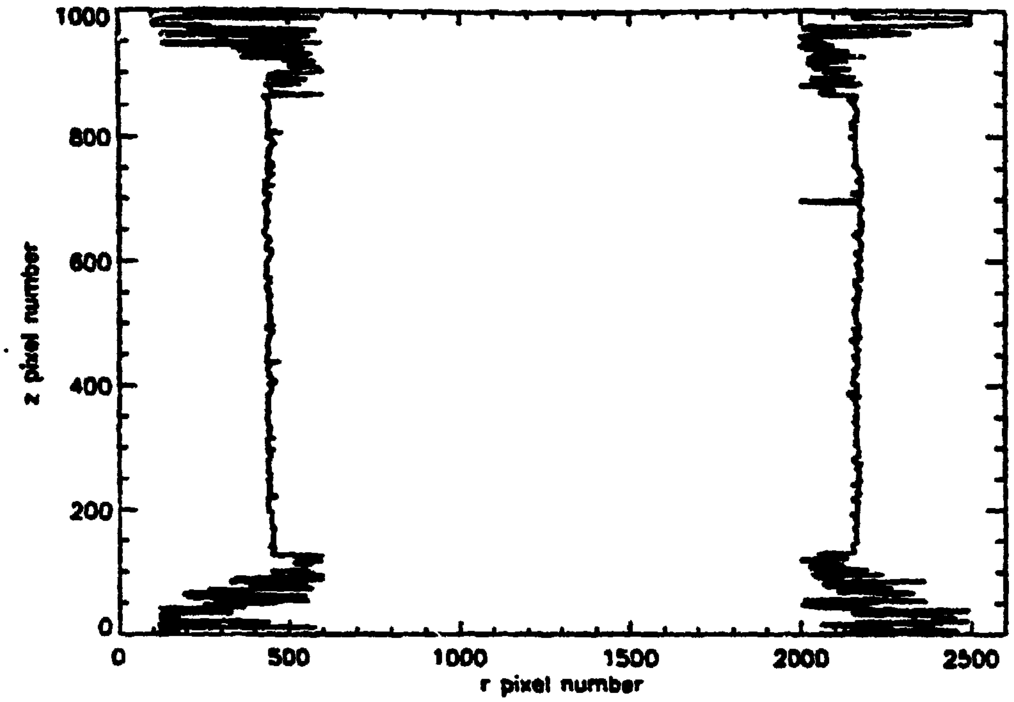

Figure 5. Inner Edge Position vs Z Pixel Number

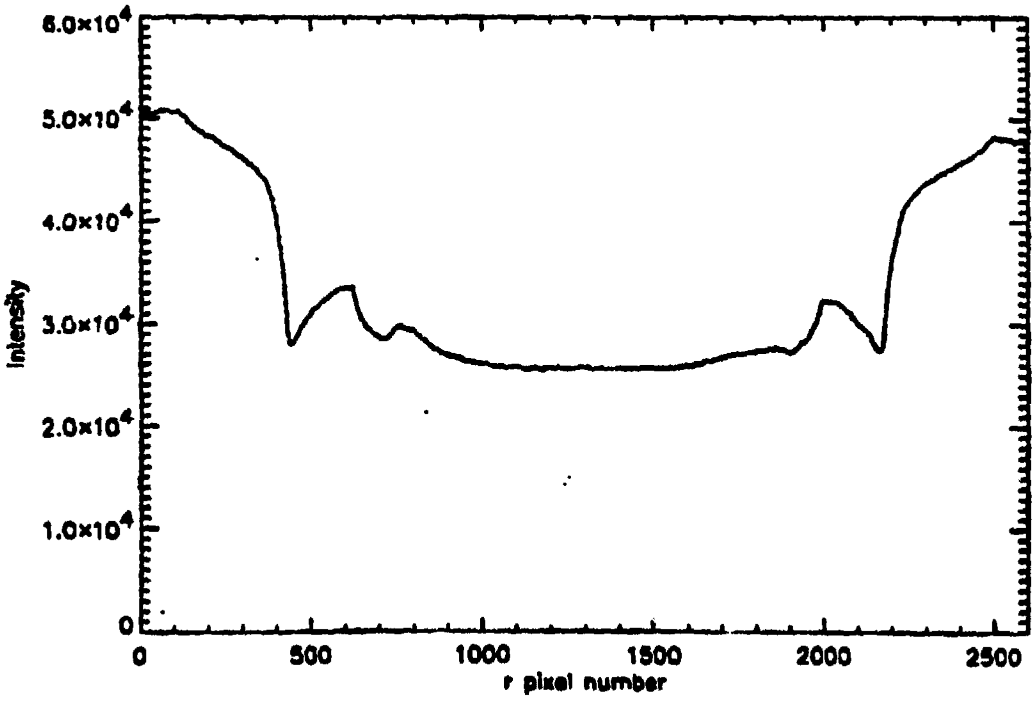

Figure 6. Averaged Line Scans

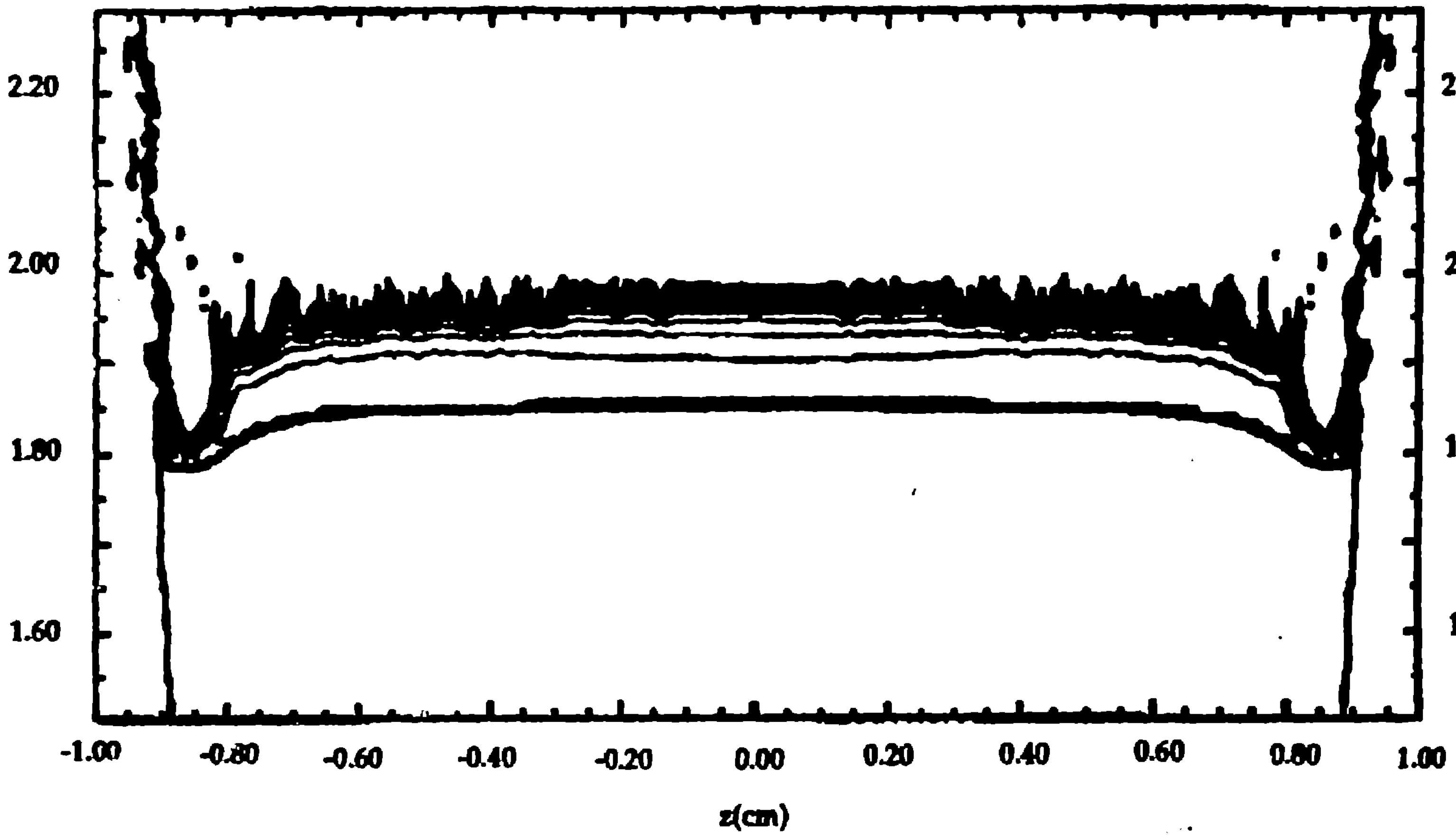

Figure 1. Predicted Density Profiles

Conclusions

- calculations predict that the growth of perturbations is suppressed until the liner starts to melt;
- the presence of a plastically deforming solid inner layer is predicted to suppresses instability growth in an overlying, unstable liquid layer;
- in the absence significant of instability growth, the liner - electrode contact is maintained and well behaved;
- the outside of the liner is unstable after melt begins;
- perturbations in the outer liquid layers grow until stabilized (presumably by an inner solid layer);
- the front edge of the liner remains undeformed and straight to better than 140 - 170 μm;
- the density at the front edge appears to be sharp